Novel Leptonic QED Effects at the JLab Heavy-Photon Probe Experiment

Atoms in Flight

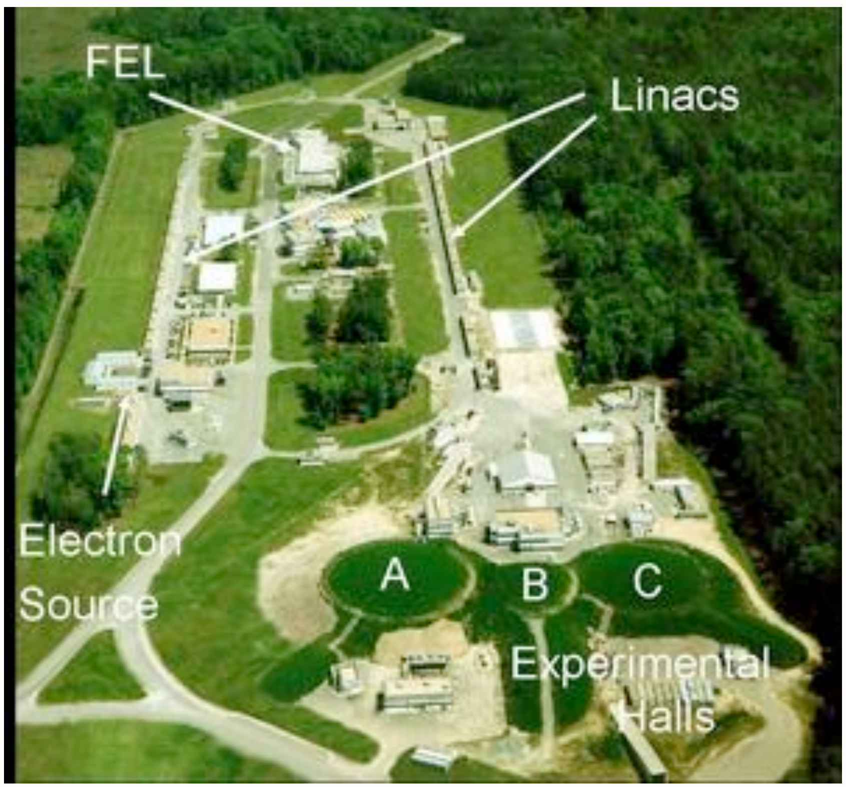

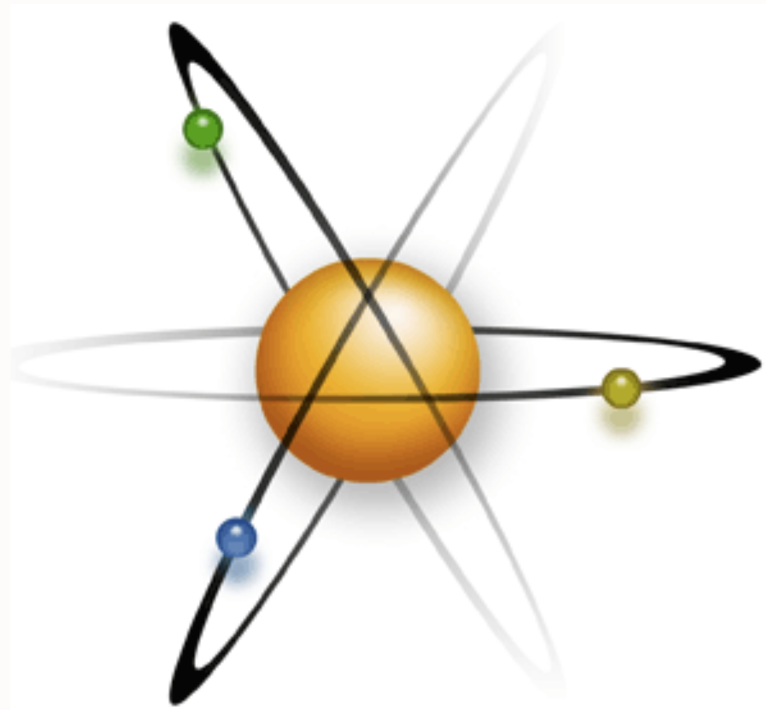

Thanks to John Jaros, Rich Lebed, Guy Ron

Indirect Dark Matter Searches in the Light of ATIC, FERMI, EGRET and PAMELA

W. de Boer

Institut für Experimentelle Kernphysik
KIT, D-76131 Karlsruhe, Germany

arXiv:0910.2601

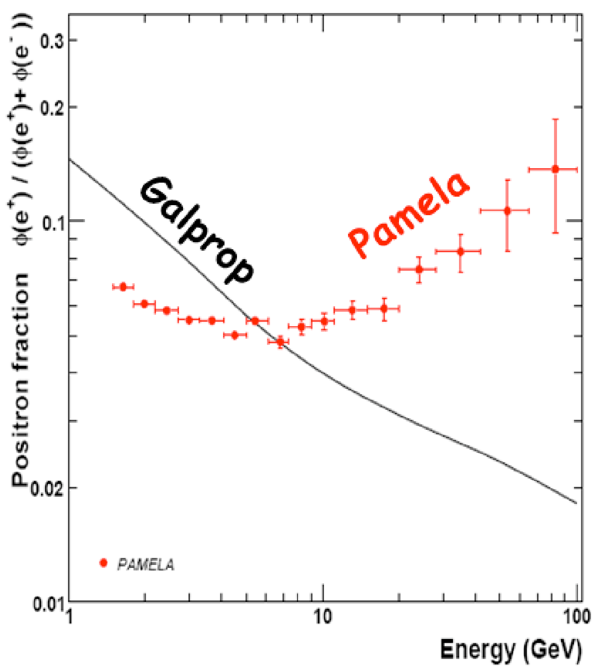

Positron fraction as measured by PAMELA in comparison with the GALPROP prediction.

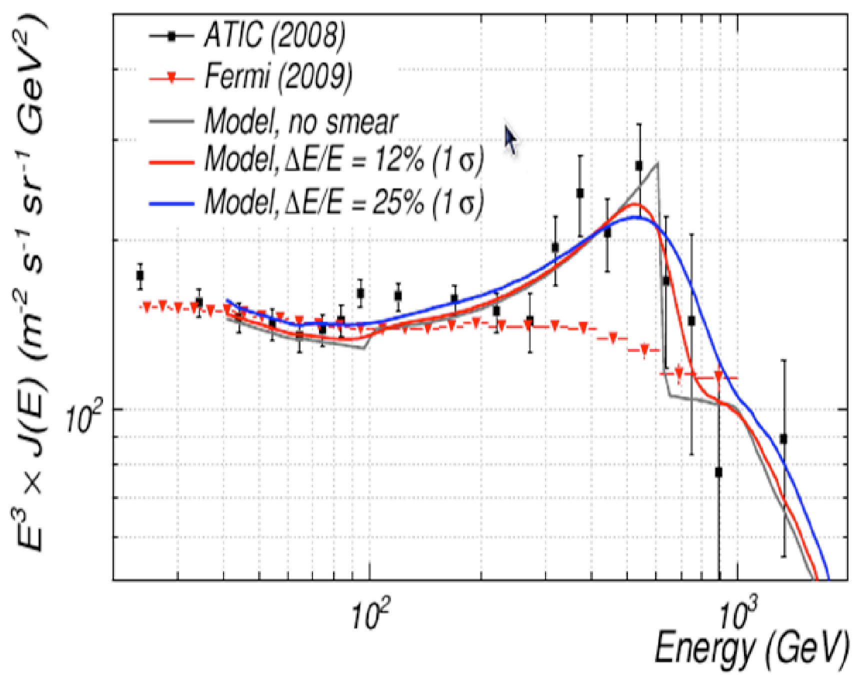

Spectrum of electrons+positrons from FERMI and ATIC.

Weakly-Coupled Heavy Photons?

Novel Lepton Physics Studies in electron-nucleus reactions

Use JLab 4 GeV Intense Electron Beam

- Production of True Muonium $[\mu^+\mu^-]$
- Production of Relativistic Muonium $[\mu^+e^-]$
- Test All-Orders Bethe-Maximon Formula for Pair Production
- Lepton Charge Asymmetry
- Test Landau-Pomeranchuk-Migdal (LPM) Effect

Why measure Bethe-Heitler/Trident Processes?

- **Test exact all-orders Bethe-Maximon formula**
- **Test lepton\anti-lepton asymmetries**
- **Compton Effect: Spacelike and Timelike DVCS**
- **Two-photon corrections -- origin of Rosenbluth breakdown?**
- **Relativistic positronium, muonium, true muonium in flight**
- **Dissociation: LFWFs, Transparency, LPM**
- **Proton size measurements; electron screening effect**
- **Muon-Proton anomaly?**
- **Fermi-Dirac Statistics**
- **QCD Analogs**

PHYSICAL REVIEW VOLUME 145, NUMBER 4 27 MAY 1966

Time-Like Momenta in Quantum Electrodynamics*

STANLEY J. BRODSKY AND SAMUEL C. C. TING
Department of Physics, Columbia University, New York, New York

(Received 6 January 1966)

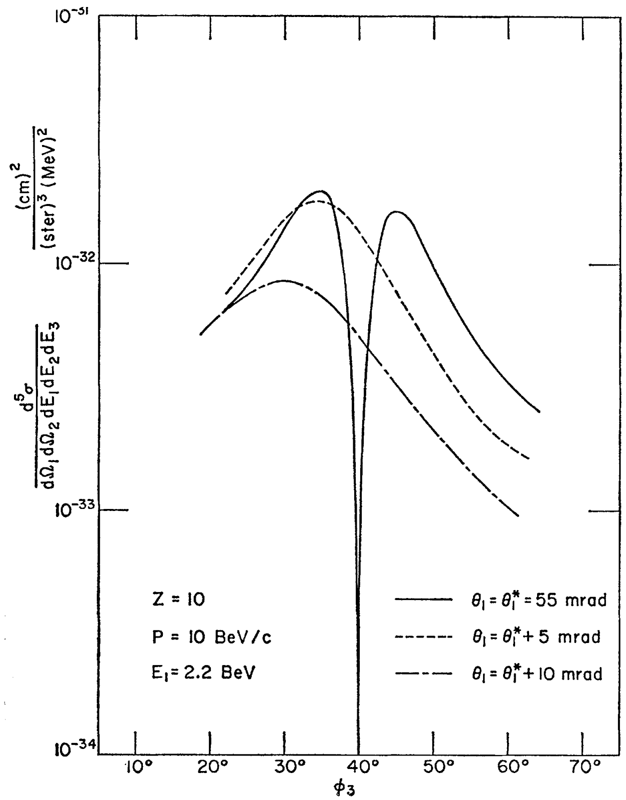

Compute each helicity amplitude using spinor representations

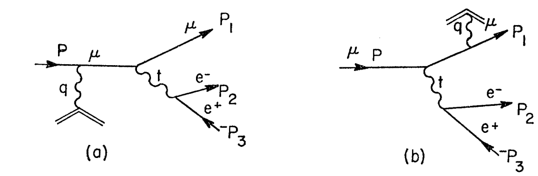

$$\ell^- Z \to \ell^- \ell^- \ell^+ Z$$

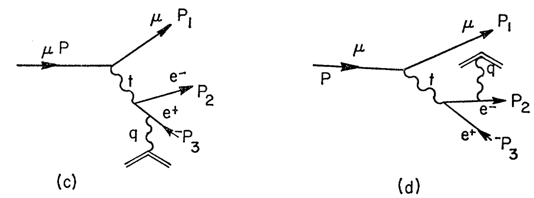

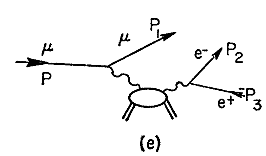

Doubly Virtual Compton Scattering

Muon Tridents

$$\mu^- Z \to \mu^- \mu^- \mu^+ Z$$

$$\frac{d^5\sigma}{dE_1 dE_2 (d\Omega)^3} = \frac{P_1 P_2 P_3}{P} \frac{Z^2\alpha^4}{2\pi^4} \times (m_\mu m_e)^2 \sum_{\text{spin}} |M_s + M_t|^2 \frac{1}{q^4},$$

Zero from chirality, J^z conservation

PHYSICAL REVIEW VOLUME 154, NUMBER 5 25 FEBRUARY 1967

High-Energy Trident Production with Definite Helicities*

J. D. Bjorken†
Stanford Linear Accelerator Center, Stanford University, Stanford, California

AND

M. C. Chen
Department of Physics, Idaho State University, Pocatello, Idaho

(Received 18 July 1966)

The high-energy large-scale-angle limit of the completely differential cross section for the process $e^- + Z \to e^- + e^+ + e^- + Z$ (or for the process with all or some of the particles replaced by muons) is computed for arbitrary helicities of incident and final particles. This process is interesting as a test of electrodynamics and of the statistics of the muon. The formula is short and perhaps suitable for numerical integrations.

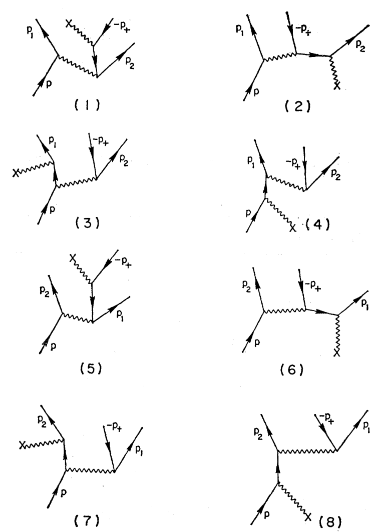

Observation of Muon Trident Production in Lead and the Statistics of the Muon*

J. J. Russell,† R. C. Sah,‡ and M. J. Tannenbaum§
Harvard University, Cambridge, Massachusetts 02138

and

W. E. Cleland||
University of Massachusetts, Amherst, Massachusetts 01002

and

D. G. Ryan and D. G. Stairs
McGill University, Montreal 110, Canada
(Received 29 October 1970)

Muons obey Fermi Statistics

We have observed the production of muon tridents in lead with an effective cross section of 51 ± 7 nb per nucleus, in agreement with the predictions of quantum electrodynamics. This measurement is sufficiently accurate that the interference term due to the presence of two identical muons in the final state is seen. The size of the measured interference term is 1.15 ± 0.25 times the value predicted for Fermi statistics.

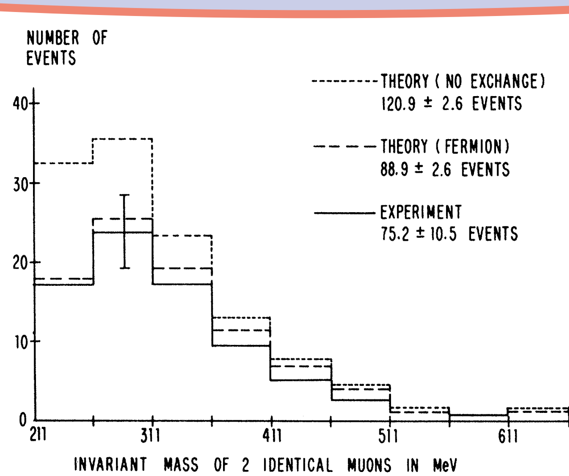

FIG. 2. Invariant-mass distribution of the two like muons in the final state.

Production of True Muonium $[\mu^+\mu^-]$

PRL **102,** 213401 (2009) PHYSICAL REVIEW LETTERS week ending 29 MAY 2009

Production of the Smallest QED Atom: True Muonium ($\mu^+\mu^-$)

Stanley J. Brodsky*

SLAC National Accelerator Laboratory, Stanford University, Stanford, California 94309, USA

Richard F. Lebed†

Department of Physics, Arizona State University, Tempe, Arizona 85287-1504, USA

(Received 22 April 2009; published 26 May 2009)

Rydberg Levels and Decays

$$\tau(n^3S_1 \to e^+e^-) = \frac{6\hbar n^3}{\alpha^5 mc^2}, \qquad \tau(n^1S_0 \to \gamma\gamma) = \frac{2\hbar n^3}{\alpha^5 mc^2},$$

$$\tau(2P \to 1S) = \left(\tfrac{3}{2}\right)^8 \frac{2\hbar}{\alpha^5 mc^2}, \qquad \tau(3S \to 2P) = \left(\tfrac{5}{2}\right)^9 \frac{4\hbar}{3\alpha^5 mc^2},$$

$$\frac{\tau(n^3S_1 \to e^+e^-)}{\tau(n^1S_0 \to \gamma\gamma)} = 3, \qquad \frac{\tau(2P \to 1S)}{\tau(n^1S_0 \to \gamma\gamma)} = \left(\tfrac{3}{2}\right)^8 \frac{1}{n^3} = \frac{25.6}{n^3},$$

$$\frac{\tau(3S \to 2P)}{\tau(2P \to 1S)} = \left(\tfrac{5}{3}\right)^9 = 99.2.$$

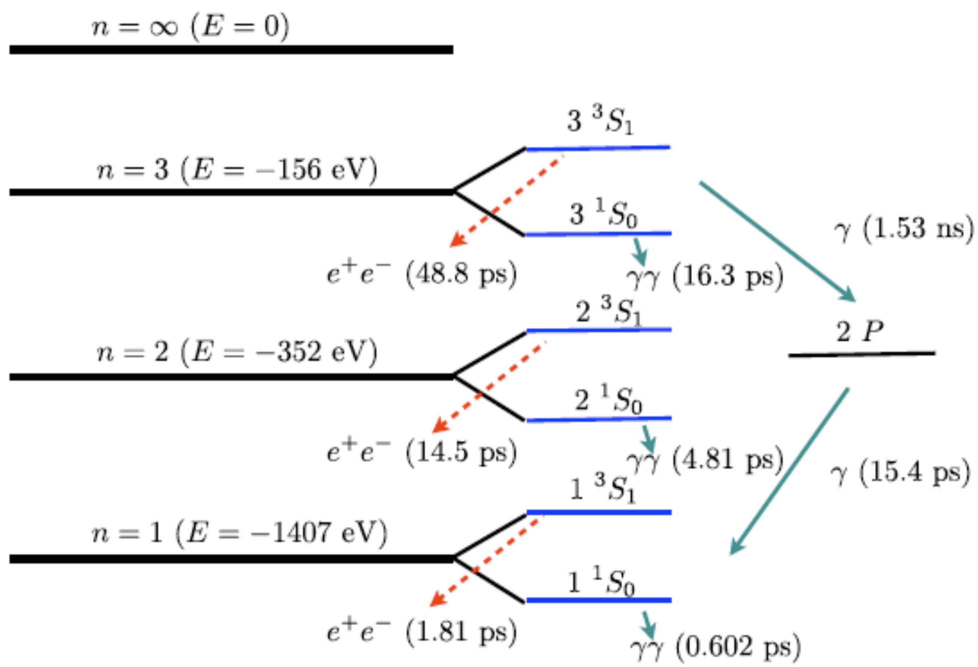

Production of bound triplet mu+ mu- system in collisions of electrons with atoms.
N. Arteaga-Romero, C. Carimalo, (Paris U., VI-VII) , V.G. Serbo, (Paris U., VI-VII & Novosibirsk State U.) . Jan 2000. 10pp.
Published in **Phys.Rev. A62:032501, 2000**.
e-Print: **hep-ph/0001278**

True Muonium

Lebed, sjb

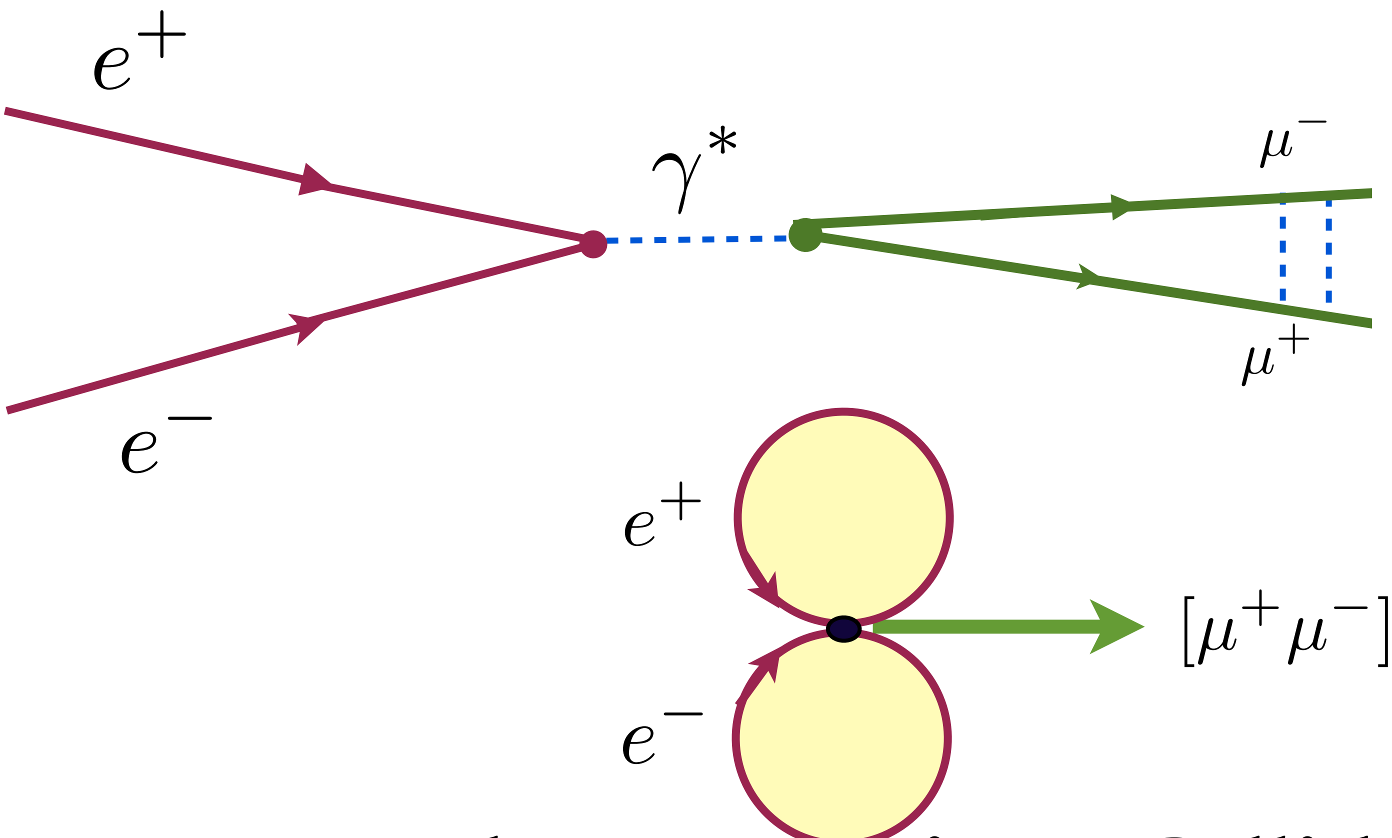

Electron-Positron Collider:
Bj: FISR (Fool's Intersecting Storage Ring) Frame

• Production of True Muonium at JLab $[\mu^+\mu^-]$

$$eZ \to eZ[\mu^+\mu^-]_{nS} \qquad q_{min} \simeq \frac{M^2_{\mu^+\mu^-}}{\nu} \sim 10 \text{ MeV}$$

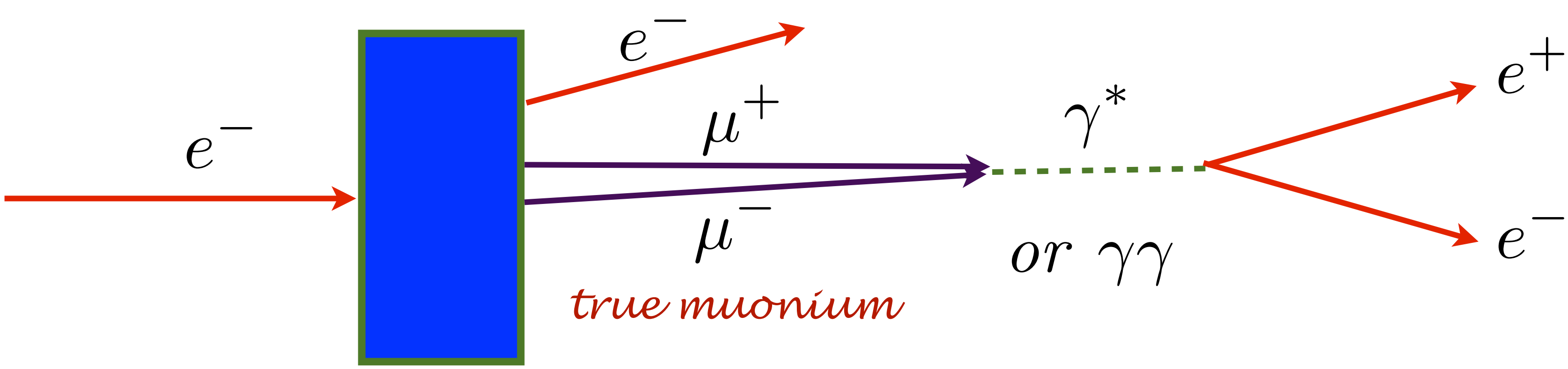

- Produces all Rydberg Levels
- Analytic connection to continuum production -- enhanced by SSS at threshold
- Gap extends in cm multiplied by Lorentz boost
- Excite/De-excite levels with external fields, lasers

• Production of True Muonium $[\mu^+\mu^-]$

$$eZ \to eZ[\mu^+\mu^-]_{nS} \qquad q_{min} \simeq \frac{M^2_{\mu^+\mu^-}}{\nu} \sim 10 \text{ MeV}$$

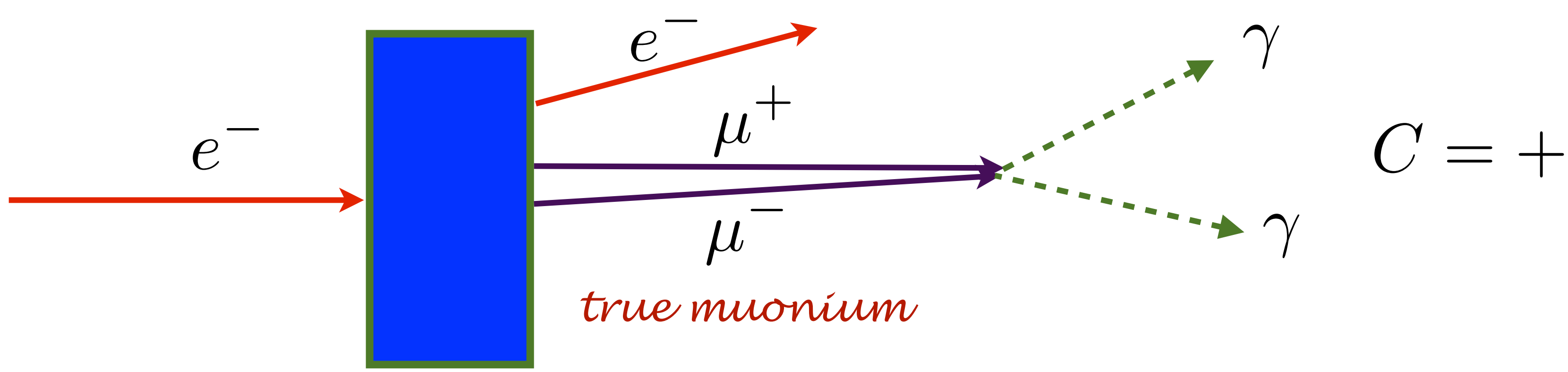

- Produces all Rydberg Levels
- Analytic connection to continuum production -- enhanced by SSS at threshold
- Gap extends in cm multiplied by Lorentz boost
- Excite/De-excite levels with external fields, lasers

• Production of True Muonium $[\mu^+\mu^-]$

$$eZ \to eZ[\mu^+\mu^-]_{nS} \qquad\qquad q_{min} \simeq \frac{M^2_{\mu^+\mu^-}}{\nu} \sim 10 \text{ MeV}$$

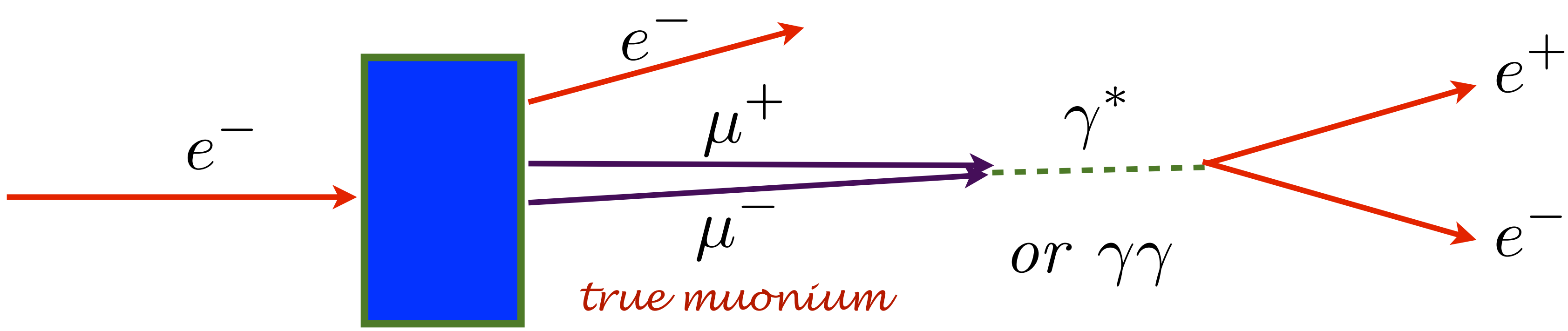

- Produces all Rydberg Levels
- Analytic connection to continuum production -- enhanced by SSS at threshold
- Gap extends in cm multiplied by Lorentz boost
- Excite/De-excite levels with external fields, lasers

• Production of True Muonium $[\mu^+\mu^-]$

$$eZ \to eZ[\mu^+\mu^-]_{nS} \qquad q_{min} \simeq \frac{M^2_{\mu^+\mu^-}}{\nu} \sim 10 \text{ MeV}$$

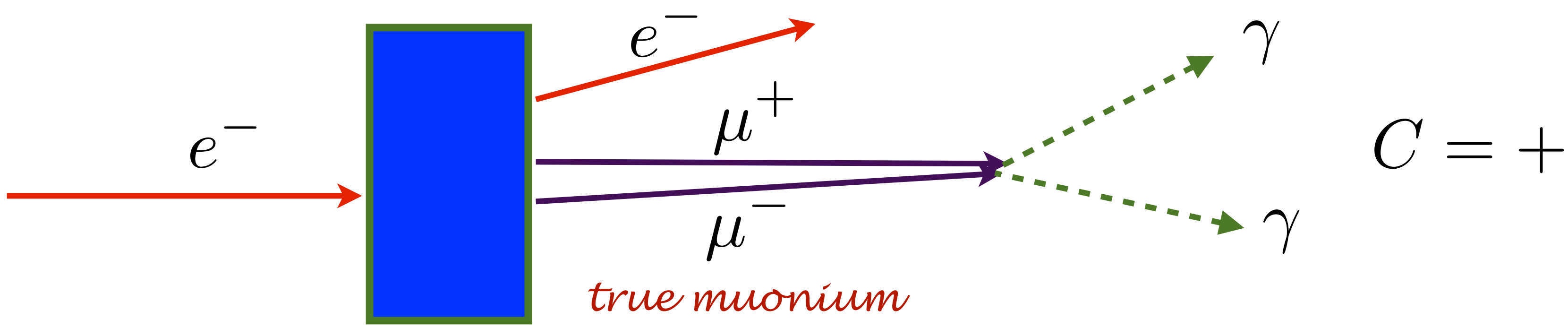

- Produces all Rydberg Levels
- Analytic connection to continuum production -- enhanced by SSS at threshold
- Gap extends in cm multiplied by Lorentz boost
- Excite/De-excite levels with external fields, lasers -- spectroscopy -- annihilation kernel

Why measure true muonium?

- First Observation
- Relativistic true muonium in flight
- Muon Anomaly
- Duality of continuum and bound states
- Dissociation: LFWFs, Front Form, Transparency, LPM
- Spectroscopy
- Lamb Shift, HFS, annihilation kernel, timelike vacuum polarization
- Zeeman from moving system through electric field
- QCD Analogs

Coulomb Enhancement of Pair Production at Threshold

$$\sigma \to \sigma S(\beta)$$

$$\beta = \sqrt{1 - \frac{4m_\ell^2}{s}}$$

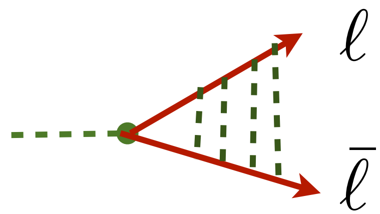

Duality of bound-state and continuum physics

$$X(\beta) = \frac{\pi\alpha\sqrt{1-\beta^2}}{\beta}$$

$$S(\beta) = \frac{X(\beta)}{1 - e^{-X(\beta)}}$$

Sommerfeld-Schwinger-Sakharov Effect

Bjorken: Analytical Connection to Rydberg Levels below Threshold

$$QCD : \pi\alpha \to \frac{4}{3}\alpha_s(\beta^2 s)$$

Kühn, Hoang, sjb

Production of True Muonium [$\mu^+\mu^-$]

PRL **102,** 213401 (2009) PHYSICAL REVIEW LETTERS week ending 29 MAY 2009

Production of the Smallest QED Atom: True Muonium ($\mu^+\mu^-$)

Stanley J. Brodsky*
SLAC National Accelerator Laboratory, Stanford University, Stanford, California 94309, USA

Richard F. Lebed†
Department of Physics, Arizona State University, Tempe, Arizona 85287-1504, USA

(Received 22 April 2009; published 26 May 2009)

Rydberg Levels and Decays

$$\tau(n^3S_1 \to e^+e^-) = \frac{6\hbar n^3}{\alpha^5 mc^2}, \qquad \tau(n^1S_0 \to \gamma\gamma) = \frac{2\hbar n^3}{\alpha^5 mc^2},$$

$$\tau(2P \to 1S) = \left(\tfrac{3}{2}\right)^8 \frac{2\hbar}{\alpha^5 mc^2}, \qquad \tau(3S \to 2P) = \left(\tfrac{5}{2}\right)^9 \frac{4\hbar}{3\alpha^5 mc^2},$$

$$\frac{\tau(n^3S_1 \to e^+e^-)}{\tau(n^1S_0 \to \gamma\gamma)} = 3, \qquad \frac{\tau(2P \to 1S)}{\tau(n^1S_0 \to \gamma\gamma)} = \left(\tfrac{3}{2}\right)^8 \frac{1}{n^3} = \frac{25.6}{n^3},$$

$$\frac{\tau(3S \to 2P)}{\tau(2P \to 1S)} = \left(\tfrac{5}{3}\right)^9 = 99.2.$$

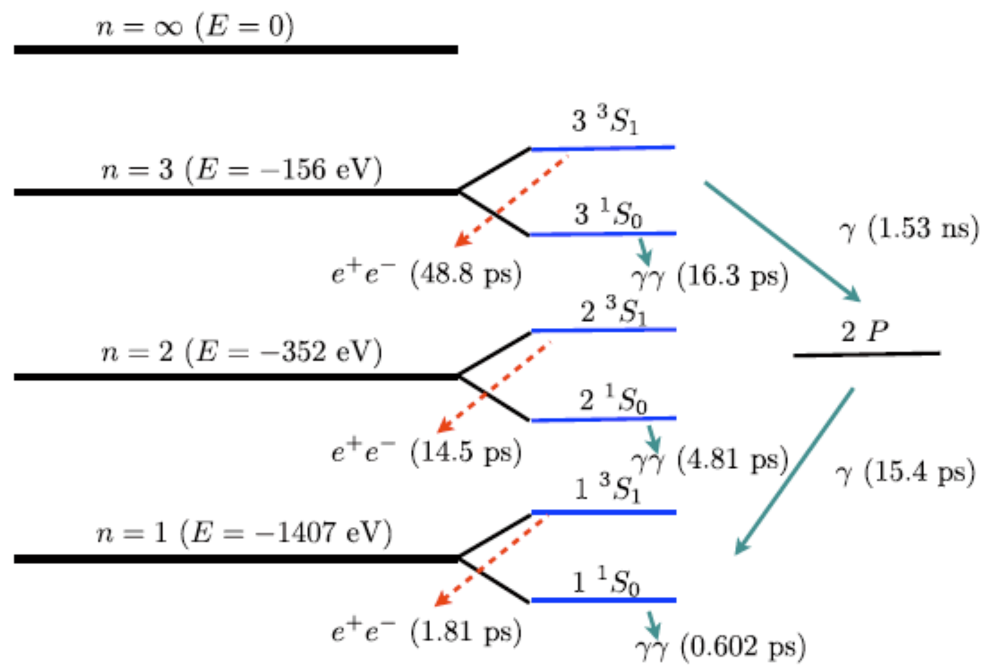

Production of bound triplet mu+ mu- system in collisions of electrons with atoms.
N. Arteaga-Romero, C. Carimalo, (Paris U., VI-VII) , V.G. Serbo, (Paris U., VI-VII & Novosibirsk State U.) . Jan 2000. 10pp.
Published in **Phys.Rev. A62:032501, 2000**.
e-Print: **hep-ph/0001278**

- **Production of True Muonium $[\mu^+\mu^-]$**

$$eZ \to eZ[\mu^+\mu^-]_{nS} \qquad q_{min} \simeq \frac{M^2_{\mu^+\mu^-}}{\nu} \sim 10 \text{ MeV}$$

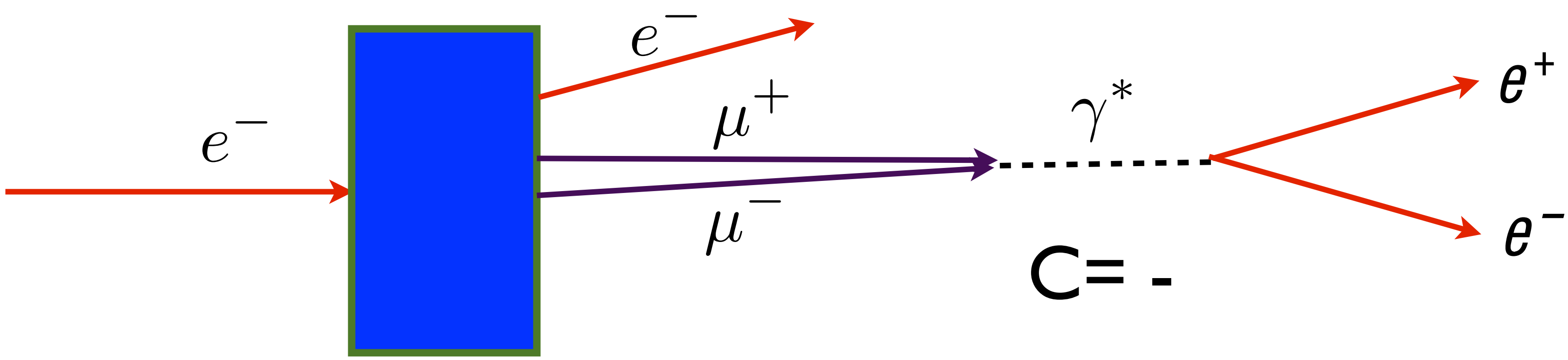

Produces all Rydberg levels within resolution

Analytic Connection to SSS - Enhanced Threshold Production

Formation of Relativistic Anti-Hydrogen

Measured at CERN-LEAR and FermiLab

Munger, Schmidt, sjb

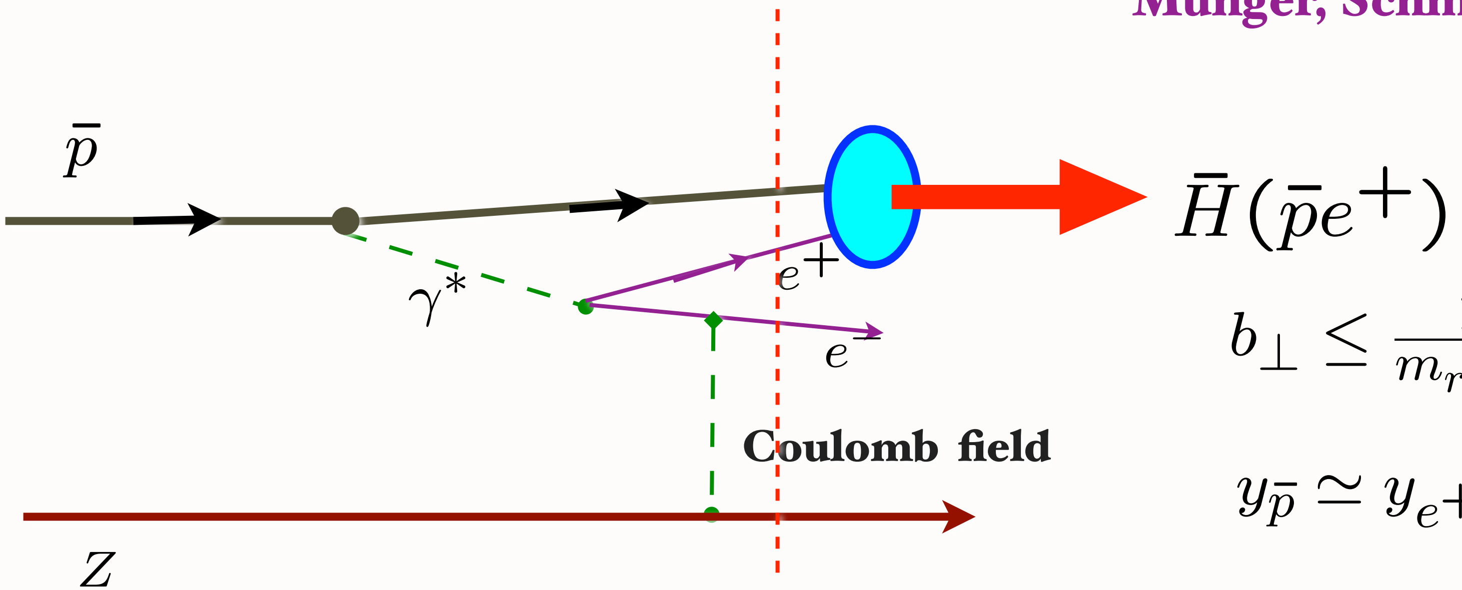

$$b_\perp \leq \frac{1}{m_{red}\alpha}$$

$$y_{\bar{p}} \simeq y_{e^+}$$

Coalescence of** off-shell **co-moving positron and antiproton

Wavefunction maximal at small impact separation and equal rapidity

"Hadronization" at the Amplitude Level

PRESSE
Organisation Européenne pour la Recherche Nucléaire
European Organization for Nuclear Research
Laboratoire Européen pour la Physique des Particules
European Laboratory for Particle Physics
Europäisches Laboratorium für Teilchenphysik
Laboratorio europeo per la fisica delle particelle

First atoms of antimatter produced at CERN

In September 1995, Prof. Walter Oelert and an international team from Jülich IKP-KFA, Erlangen-Nuernberg University, GSI Darmstadt and Genoa University succeeded for the first time in synthesising atoms of antimatter from their constituent antiparticles. Nine of these atoms were produced in collisions between antiprotons and xenon atoms over a period of three weeks. Each one remained in existence for about forty billionths of a second, travelled at nearly the speed of light over a path of ten metres and then annihilated with ordinary matter. The annihilation produced the signal which showed that the anti-atoms had been created.

Ordinary atoms consist of a number of electrons in orbit around an atomic nucleus. The hydrogen atom is the simplest atom of all; its nucleus consists of a proton, around which a single electron circulates. The recipe for anti-hydrogen is very simple - take one antiproton, bring up one anti-electron, and put the latter into orbit around the former - but it is very difficult to carry out as antiparticles do not naturally exist on earth. They can only be created in the laboratory. The experimenters whirled previously created antiprotons around the CERN* Low Energy Antiproton Ring (LEAR), passing them through a xenon gas jet each time they went around - about 3 million times each second. (see scheme of the experiment) Very occasionally, an antiproton converted a small part of its own energy into an electron and an anti-electron, usually called a positron, while passing through a xenon atom. In even rarer cases, the positron's velocity was sufficiently close to the velocity of the antiproton for the two particles to join - creating an atom of anti-hydrogen (see diagram of the principle) .

Three quarters of our universe is hydrogen and much of what we have learned about it has been found by studying ordinary hydrogen. If the behaviour of anti-hydrogen differed even in the tiniest detail from that of ordinary hydrogen, physicists would have to rethink or abandon many of the established ideas on the symmetry between matter and antimatter. Newton's historic work on gravity was supposedly prompted by watching an apple fall to earth, but would an "anti-apple" fall in the same way? It is believed that antimatter "works" under gravity in the same way as matter, but if nature has chosen otherwise, we must find out how and why.

The next step is to check whether anti hydrogen does indeed "work" just as well as ordinary hydrogen. Comparisons can be made with tremendous accuracy, as high as one part in a million trillion, and even an asymmetry on this tiny scale would have enormous consequences for our understanding of the universe. To check for such an asymmetry would mean holding the anti-atoms still, for seconds, minutes, days or weeks. The techniques needed to store antimatter are under intense development at CERN. New experiments are currently being planned, to capture antimatter in electrical and magnetic bottles or traps allowing for high precision analysis.

The first ever creation of atoms of antimatter at CERN has opened the door to the systematic exploration of the anti world.

- **Production of Relativistic Muonium [μ^+e^-]**

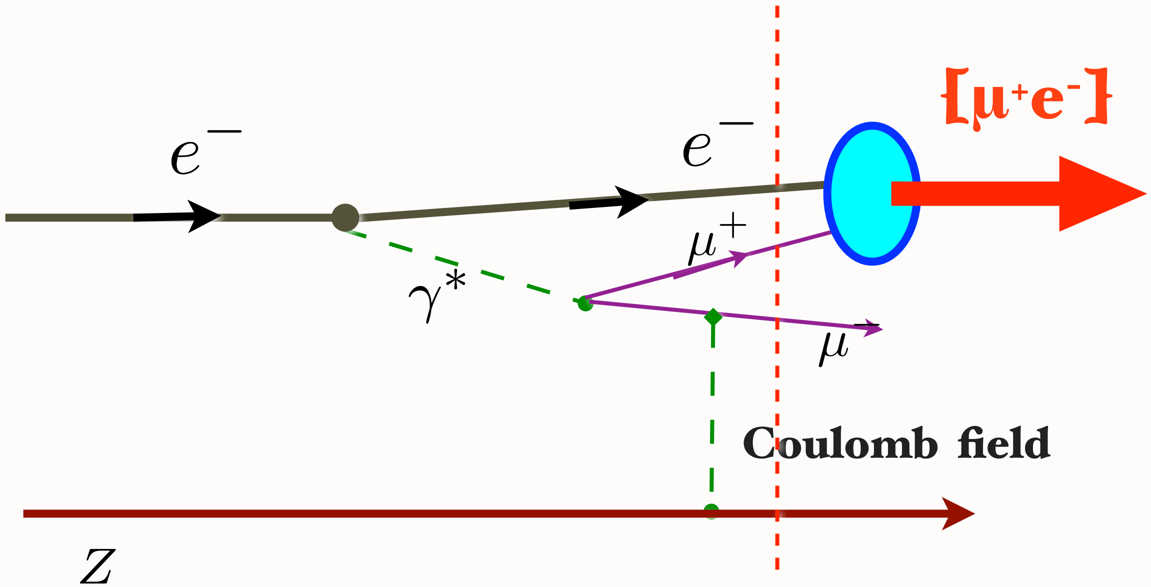

$$b_\perp \leq \frac{1}{m_{red}\alpha}$$

$$y_{\bar{p}} \simeq y_{e^+}$$

Coalescence of off-shell co-moving electron and muon

Wavefunction maximal at small impact separation and equal rapidity

"Atom Formation" at the Amplitude Level

Production of Relativistic Muonium $[\mu^+ e^-]$

- Never Observed Before?
- Measure Lamb Shift of Muonium by Robiscoe Method (Level Crossing by Induced Magnetic Field)
- Precision Tests of Time Dilation
- Dissociate to muon and electron with foils
- Flying Atoms

- **Production of Relativistic Muonium [μ⁺e⁻]**

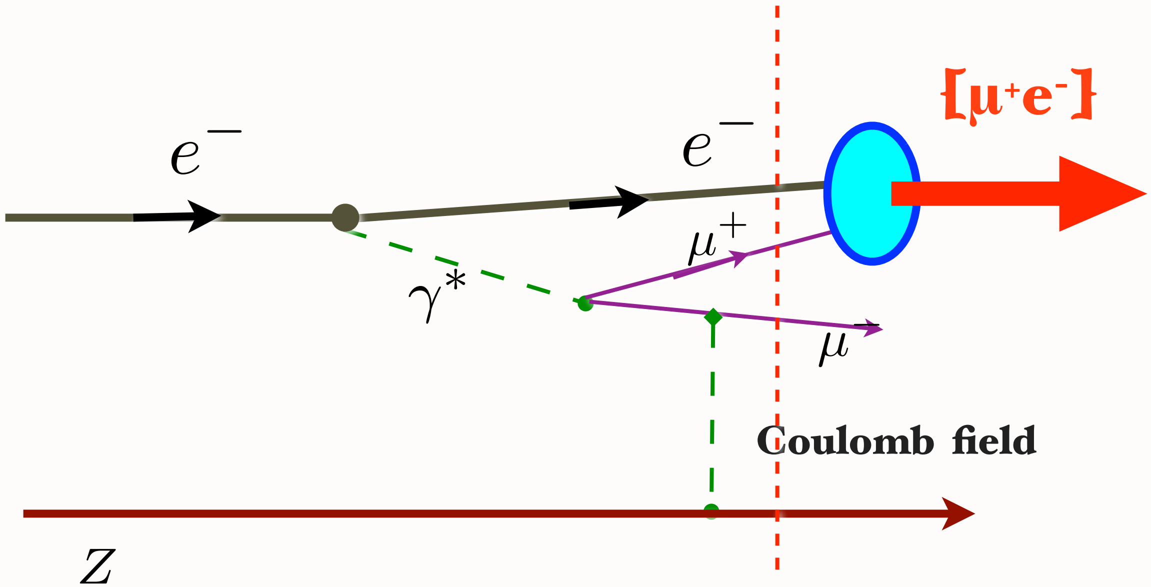

$$b_\perp \leq \frac{1}{m_{red}\alpha}$$

$$y_{\bar{p}} \simeq y_{e^+}$$

Coalescence of off-shell co-moving electron and muon

Wavefunction maximal at small impact separation and equal rapidity

"Atom Formation" at the Amplitude Level

Hadronization at the Amplitude Level

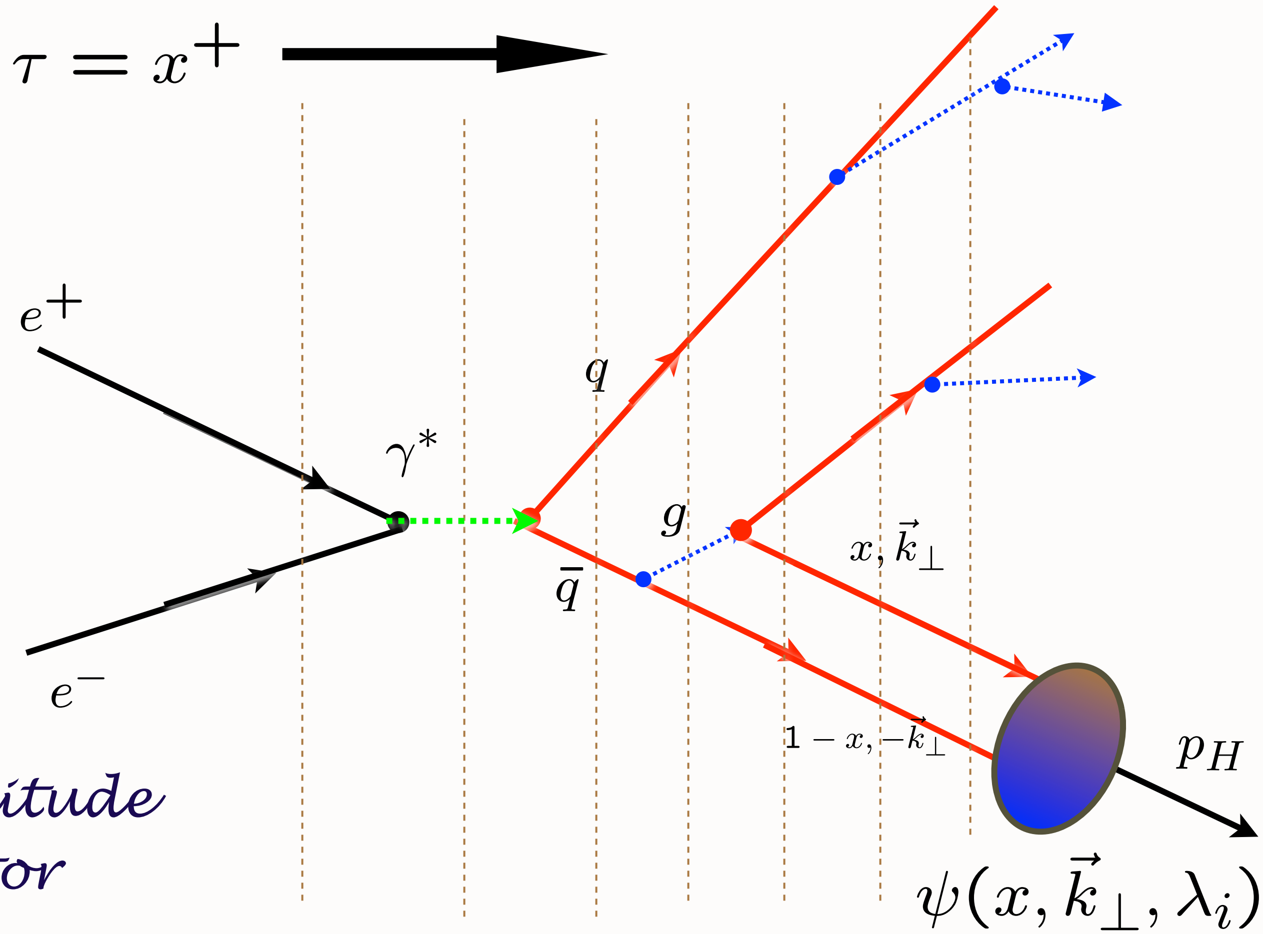

Event amplitude generator

Construct helicity amplitude using Light-Front Perturbation theory; coalesce quarks via LFWFs

Flying Atoms?

News story originally written on June 4, 1999

Artist's version of the ACE spacecraft.
Click on image for full size (24K GIF)
Courtesy of NASA

Scientists have found a possible source of the high speed atoms flying through space in the form of cosmic rays. These atoms reach velocities close to the speed of light. It was known that the source of the energy that causes the high speeds is a supernova, or exploding star. However, the exact source of the actual atoms was unknown until now.

Using an instrument aboard NASA's Advanced Composition Explorer (ACE), scientists are able to investigate the cosmic rays, and have come up with some surprising results. NASA scientists now believe the atoms are pieces of dust and gas already in space, being pushed through by the explosions.

Scientists know that a certain type of Nickel decays over time. They found atoms that have been decaying for 100,000 years. In order to decay, Nickel atoms have to be stationary. It is impossible for the atoms to be going the speed of light and decay at the same time. Scientists conclude the atoms must be made of gas and dust that was already in space.

Bethe-Salpeter Equation for Hydrogenic Atoms

$$(\not{p}_a - m_a)(\not{p}_b - m_b)|N> = G|N>$$

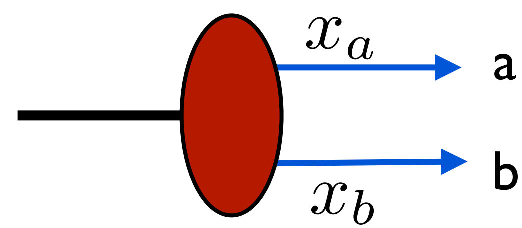

$$p_a^\mu + p_b^\mu = P^\mu = (E_N, \vec{P})$$

an eigenvalue problem for $P^0 = E_N = \sqrt{M_N^2 + \vec{P}^2}$

$$(i\not{\partial}_a - m_a)(i\not{\partial}_b - m_b)\chi_N(x_a, x_b) = (G\chi_N)(x_a, x_b)$$

In momentum space: $\quad P = p_a + p_b \qquad p = \tau_b p_a - \tau_a p_b$

$$\boxed{\begin{aligned}[\gamma^{(a)} \cdot (\tau_a P + p) - m_a][\gamma^{(b)} \cdot (\tau_b P - p) - m_b]\Psi_N(p, P) \\ = \int d^4p' G(p, p'; P)\Psi_N(p', P)\end{aligned}}$$

$$\tau_a = \frac{m_a}{m_a + m_b} \qquad \tau_b = \frac{m_b}{m_a + m_b}$$

Bethe-Salpeter Theory of Hydrogenic Atoms

Bethe–Salpeter Equation

$$(\not{p}_e - m_e)(\not{p}_p - m_p)\,\chi = G\chi$$

$$G = G_{1\gamma} \quad + \quad G_{\text{CROSSED}} \quad + \quad G_{\text{VAC.POL.}} \quad + \quad G_{\text{SELF ENERGY}} \quad + \quad G_{\text{NUC-POL}} + \cdots$$

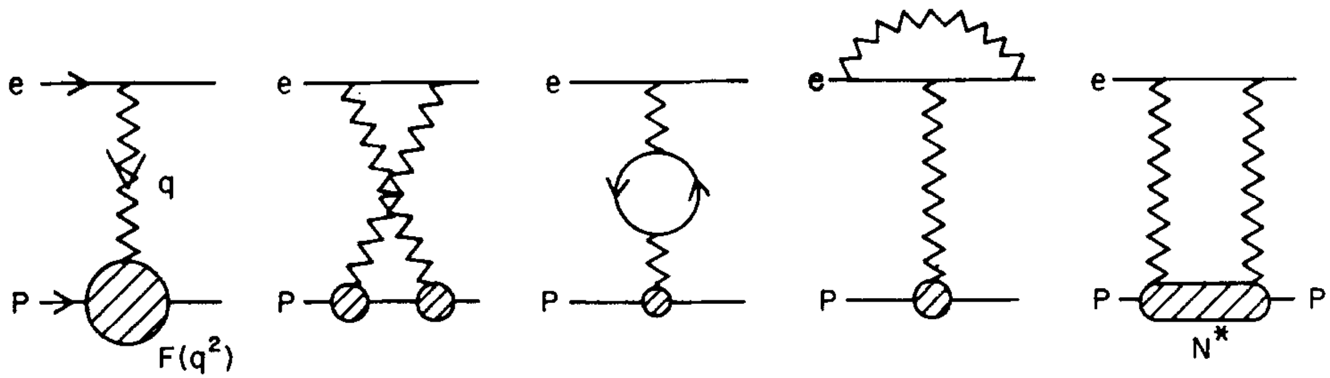

$$G_{1\gamma} = G_{\text{COULOMB}} + G_{\text{TRANSVERSE}}$$

$$-\epsilon_\mu \frac{1}{q^2}\epsilon^\mu = \epsilon_0 \frac{1}{\mathbf{q}^2}\epsilon_0 + \sum_{\substack{\text{TRAN}\\ i=1,2}} \epsilon_i \frac{1}{q^2}\epsilon_i$$

G_{COULOMB} → Schrödinger equation, proton finite size correction

$+\ G_{\text{TRANS}}$ → reduced mass corrections, HFS splittings

$+\ G^{(\text{all})}_{\text{CROSSED}}$ → Dirac equation, relativistic reduced mass correction

$+\ G_{\text{VAC-POL}} + G_{\text{SELF ENERGY}}$ → Lamb shift, radiative corrections to HFS

$+\ G_{\text{NUC-POL}}$ → correction to HFS

Features of Bethe-Salpeter Equation

- **Exact Bound-State Formalism for QED if one includes all 2PI kernels**
- **Eigenvalues give complete spectrum, bound state and continuum**
- **Relativistic, Frame Independent**
- **Feynman virtualities:** $p_i^2 \neq m_i^2$
- **Reduces to Dirac Coulomb Equation if one includes all crossed graph 2PI kernels**
- **Matrix Elements of electromagnetic current from sum of all 2PI contributions**
- **Normalization of Bethe-Salpeter Wavefunctions also requires sum of all 2PI kernels**
- **n-body formulation difficult**
- **No cluster decomposition theorem**

Solution to Salpeter Equation in CM frame

Total spin S,
Projection S^z = M

$$\varphi_{\mathscr{M}}(\mathbf{x}_a\,,\mathbf{x}_b\,,X^0)_{SM} = \int \frac{d^3p}{(2\pi)^{3/2}} \left(\frac{p_a{}^0+m_a}{2p_a{}^0}\frac{p_b{}^0+m_b}{2p_b{}^0}\right)^{1/2} \begin{pmatrix} 1 \\ \dfrac{\boldsymbol{\sigma}_a\cdot\mathbf{p}}{2m_a+k_a}\end{pmatrix} \otimes \begin{pmatrix} 1 \\ -\dfrac{\boldsymbol{\sigma}_b\cdot\mathbf{p}}{2m_b+k_b}\end{pmatrix}$$

$$\times\ \phi_{\mathscr{M}}(\mathbf{p})\,\chi_{SM}e^{i\mathbf{p}\cdot\mathbf{x}-i\mathscr{M}X^0}$$

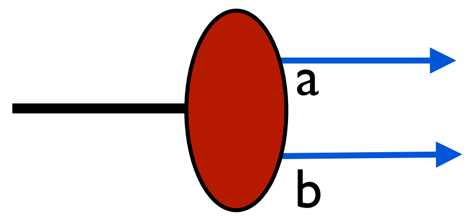

$$k_{a,b} \equiv -\tau_{b,a}(U+W)$$

$$\int d^3x_a\,d^3x_b\,\varphi_{\mathscr{M}}(\mathbf{x}_a\,,\mathbf{x}_b)^\dagger\,(\Lambda_{++}-\Lambda_{--})\,\varphi_{\mathscr{M}}(\mathbf{x}_a\,,\mathbf{x}_b) = 1$$

$$\int d^3p\,|\,\phi_{\mathscr{M}}(\mathbf{p})|^2 = 1.$$

$$\chi^{\alpha\beta}_{\mathscr{M}}(x_a\,,x_b)_{SM} = \langle 0\,|\,T(\psi_a{}^\alpha(x_a)\,\psi_b{}^\beta(x_b))\,|\,0\mathscr{M}SM\rangle$$

Lorentz Boost

$$\Phi_{\mathcal{M}}(x_a, x_b)_{SM} =< 0|T(\psi(x_a)\psi_b(x_b)|\vec{P} = \vec{0}, \mathcal{M}, S, M >$$

$$\Phi_{E,\vec{P}}(x'_a, x'_b)_{SM} = S_a(\Lambda)S_b(\Lambda)\Phi_{\mathcal{M}}(x_a, x_b)_{SM}$$

$$S_a(\Lambda) = \sqrt{\frac{E+\mathcal{M}}{2\mathcal{M}}}\left(1 + \frac{\vec{\alpha}_a \cdot \vec{P}}{\mathcal{M}+E}\right)$$

$$S_a(\Lambda)u(0) = u(p) = \sqrt{\frac{p^0+m}{2m}}\begin{pmatrix} 1 \\ \frac{\sigma \cdot p}{p^0+m} \end{pmatrix}\chi$$

Single particle wave-packet

$$\phi(x) = \int \frac{d^3p}{(2\pi)^{3/2}} \sqrt{\frac{m}{p^0}}\, u(p)\, \phi(p)\, e^{-ip.x}$$

$$u(p) = \sqrt{\frac{p^0+m}{2m}} \begin{pmatrix} 1 \\ \dfrac{\boldsymbol{\sigma}\cdot\mathbf{p}}{p^0+m} \end{pmatrix} \chi.$$

Guess wavefunction for moving bound state

$$\varphi_{E\mathbf{P}}(\mathbf{x}_a \quad \mathbf{x}_b\,,\, X^0)_{SM}$$

$$= \frac{E+\mathcal{M}}{2\mathcal{M}} \int \frac{d^3p}{(2\pi)^{3/2}} \left(\frac{p_a{}^0+m_a}{2p_a{}^0}\, \frac{p_b{}^0+m_b}{2p_b{}^0}\right)^{1/2}$$

$$\times \begin{pmatrix} 1 \\ \boldsymbol{\sigma}_a\cdot\left(\dfrac{\mathbf{P}}{\mathcal{M}+E}+\dfrac{\mathbf{p}}{2m_a+k_a}\right) \end{pmatrix} \otimes \begin{pmatrix} 1 \\ \boldsymbol{\sigma}_b\cdot\left(\dfrac{\mathbf{P}}{\mathcal{M}+E}-\dfrac{\mathbf{p}}{2m_b+k_b}\right) \end{pmatrix}$$

$$\times\ \phi_{\mathcal{M}}(\mathbf{p})\, \chi_{SM}\, \exp[i\mathbf{p}\cdot\tilde{\mathbf{x}}+i\mathbf{P}\cdot\mathbf{X}]\, \exp[-iEX^0].$$

$$\tilde{\mathbf{x}} = \mathbf{x}+(\gamma-1)\,\hat{\mathbf{V}}\hat{\mathbf{V}}\cdot\mathbf{x} \quad ; \quad p^0_{a,b} = \sqrt{\mathbf{p}^2+m^2_{a,b}}\,, \quad k_{a,b} \equiv -\tau_{b,a}(U+W)$$

Single particle wave-packet

$$\phi(x) = \int \frac{d^3p}{(2\pi)^{3/2}} \sqrt{\frac{m}{p^0}}\, u(p)\, \phi(p)\, e^{-ip.x}$$

$$u(p) = \sqrt{\frac{p^0+m}{2m}} \begin{pmatrix} 1 \\ \dfrac{\boldsymbol{\sigma}\cdot\mathbf{p}}{p^0+m} \end{pmatrix} \chi.$$

Correct wavefunction for moving bound state

Not product of independent boosts!

$$\begin{aligned}
&\varphi_{E\mathbf{P}}(\mathbf{x}_a \;\; \mathbf{x}_b\,, X^0)_{SM} \\
&= \frac{E+\mathcal{M}}{2\mathcal{M}} \int \frac{d^3p}{(2\pi)^{3/2}} \left(\frac{p_a{}^0+m_a}{2p_a{}^0}\,\frac{p_b{}^0+m_b}{2p_b{}^0}\right)^{1/2} \\
&\quad \times \begin{pmatrix} 1 + \dfrac{\boldsymbol{\sigma}_a\cdot\mathbf{P}}{\mathcal{M}+E}\,\dfrac{\boldsymbol{\sigma}_a\cdot\mathbf{p}}{2m_a+k_a} \\ \boldsymbol{\sigma}_a\cdot\left(\dfrac{\mathbf{P}}{\mathcal{M}+E}+\dfrac{\mathbf{p}}{2m_a+k_a}\right) \end{pmatrix} \otimes \begin{pmatrix} 1 - \dfrac{\boldsymbol{\sigma}_b\cdot\mathbf{P}}{\mathcal{M}+E}\,\dfrac{\boldsymbol{\sigma}_b\cdot\mathbf{p}}{2m_b+k_b} \\ \boldsymbol{\sigma}_b\cdot\left(\dfrac{\mathbf{P}}{\mathcal{M}+E}-\dfrac{\mathbf{p}}{2m_b+k_b}\right) \end{pmatrix} \\
&\quad \times \phi_{\mathcal{M}}(\mathbf{p})\, \chi_{SM} \exp[i\mathbf{p}\cdot\tilde{\mathbf{x}} + i\mathbf{P}\cdot\mathbf{X}] \exp[-iEX^0].
\end{aligned}$$

$$\tilde{\mathbf{x}} = \mathbf{x} + (\gamma-1)\,\hat{\mathbf{V}}\hat{\mathbf{V}}\cdot\mathbf{x} \;; \quad p^0_{a,b} = \sqrt{\mathbf{p}^2+m^2_{a,b}}\,, \quad k_{a,b} \equiv -\tau_{b,a}(U+W).$$

Boost of a Composite System

J. Primack and sjb

- Boost is not product of independent boosts of constituents since constituents are already moving
- Only known at weak binding
- Dirac: Boosts are dynamical in instant form
- Correct form needed to prove Low Energy Theorem for Compton scattering and Drell-Hearn Gerasimov Sum Rule

Dirac's Amazing Idea: The "Front Form"

Evolve in light-front time

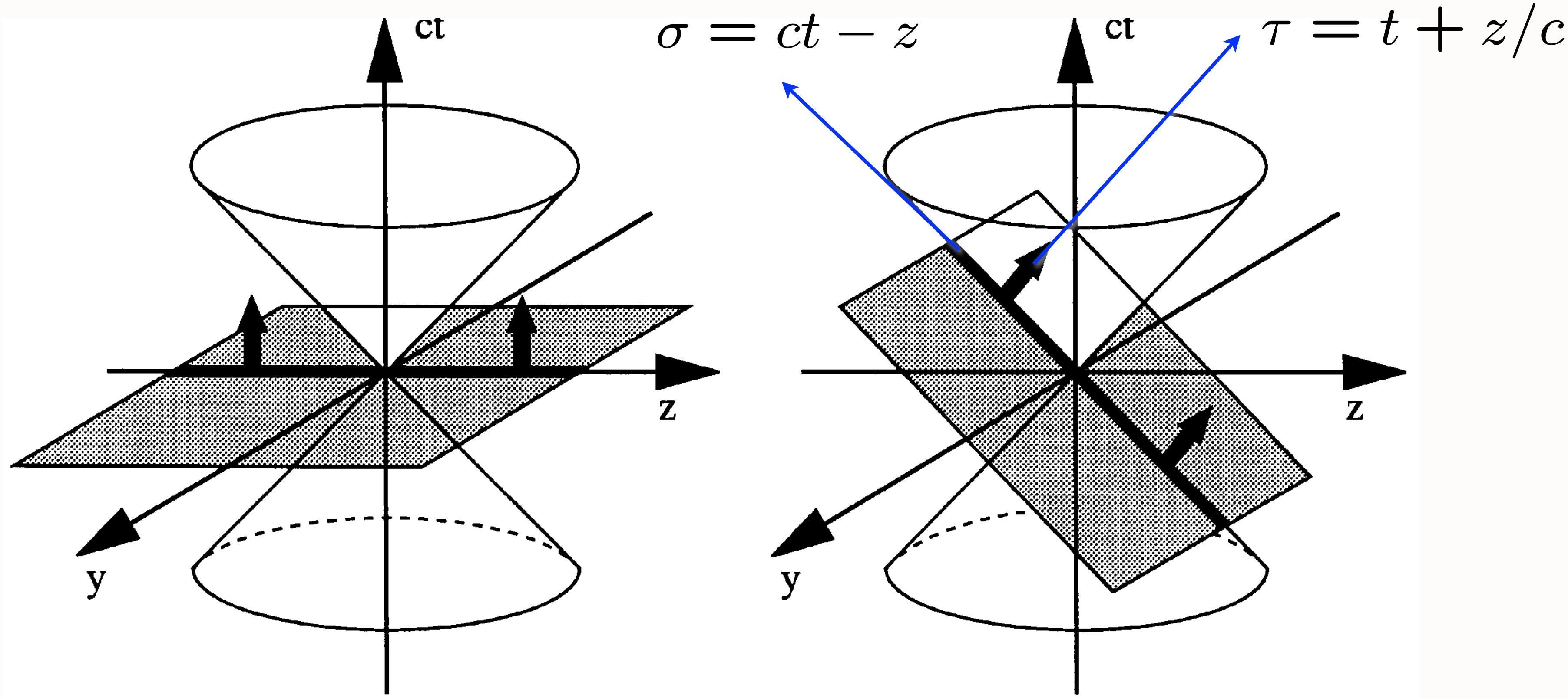

Instant Form

Front Form

Each element of flash photograph illuminated at same LF time

$$\tau = t + z/c$$

Evolve in LF time

$$P^- = i\frac{d}{d\tau}$$

Eigenstate -- independent of τ

Causally-Connected Domains

HELEN BRADLEY - PHOTOGRAPHY

'Tis a mistake / Time flies not
It only hovers on the wing
Once born the moment dies not
'tis an immortal thing

Montgomery

Light-Front Wavefunctions: rigorous representation of composite systems in quantum field theory

Fixed $\tau = t + z/c$

$$x = \frac{k^+}{P^+} = \frac{k^0 + k^3}{P^0 + P^3}$$

$P^+, \vec{P}_\perp$

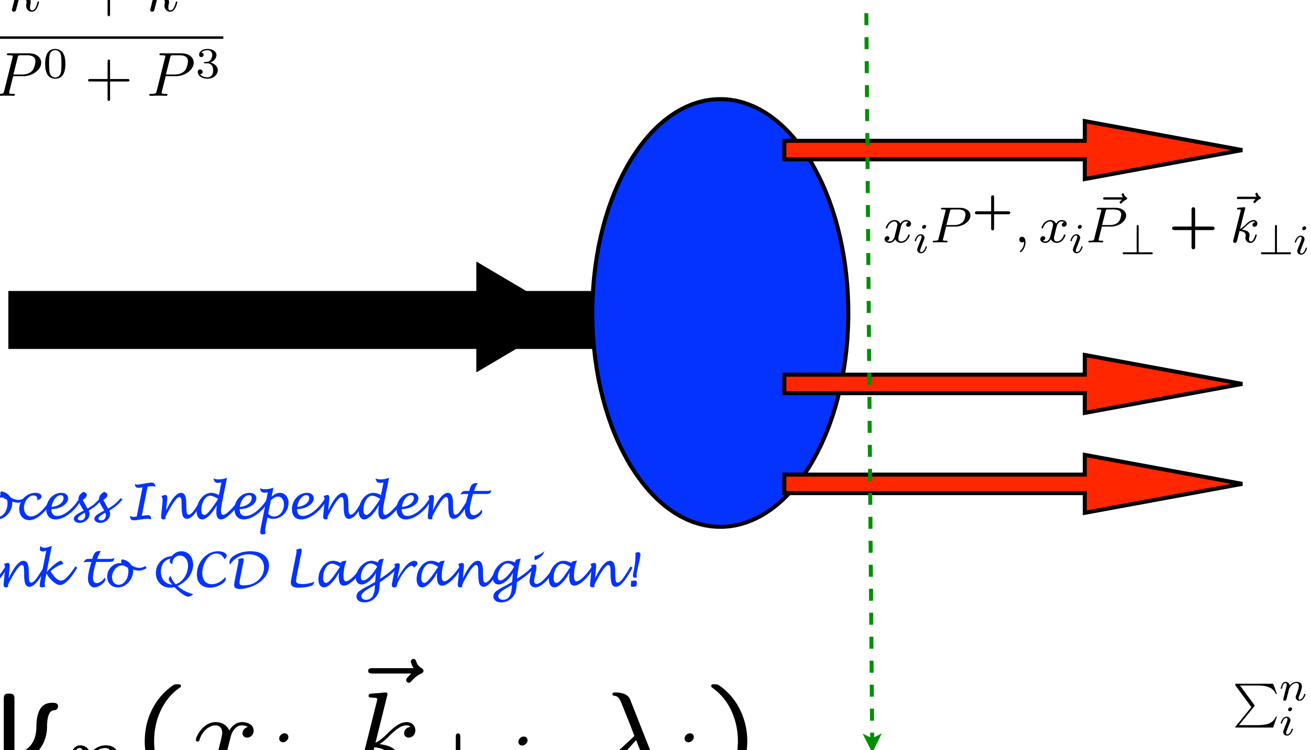

Process Independent
Direct Link to QCD Lagrangian!

$$\Psi_n(x_i, \vec{k}_{\perp i}, \lambda_i)$$

$\sum_i^n x_i = 1$

$\sum_i^n \vec{k}_{\perp i} = \vec{0}_\perp$

Invariant under boosts! Independent of P^μ

Apply Front Form to Relativistic Atoms

Angular Momentum on the Light-Front

$$J^z = \sum_{i=1}^{n} s_i^z + \sum_{j=1}^{n-1} l_j^z.$$

Conserved
LF Fock state by Fock State!

LF Spin Sum Rule

$$l_j^z = -\mathrm{i}\left(k_j^1 \frac{\partial}{\partial k_j^2} - k_j^2 \frac{\partial}{\partial k_j^1}\right)$$

n-1 orbital angular momenta

Orbital angular momentum is a property of Light-Front Wavefunctions

Nonzero Anomalous Moment -->Nonzero orbital angular momentum

Quantum Mechanics: Uncertainty in p, x, spin

Relativistic Quantum Field Theory: Uncertainty in particle number n

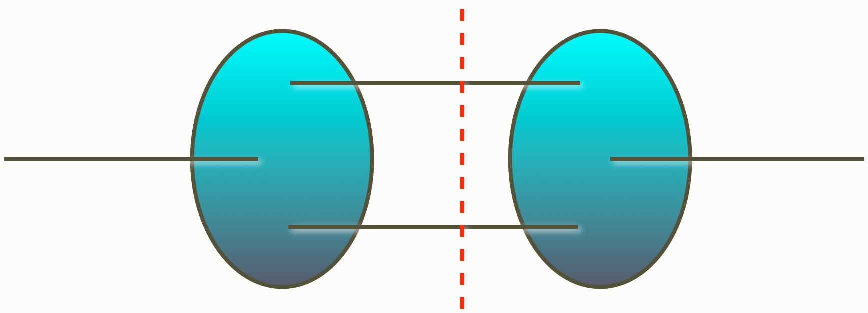

Positronium n=2

e^+e^-

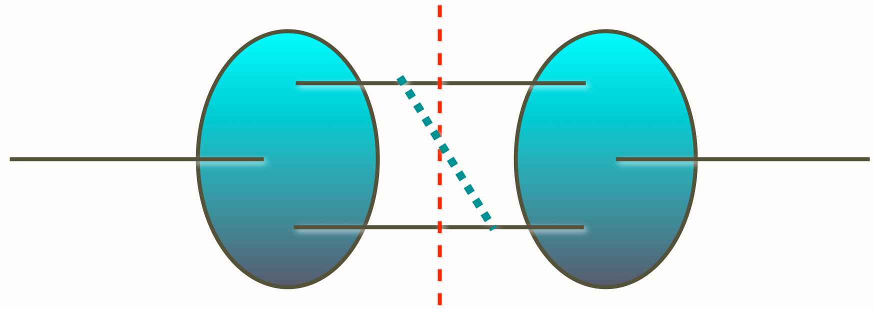

Hyperfine splitting n=3

$e^+e^-\gamma$

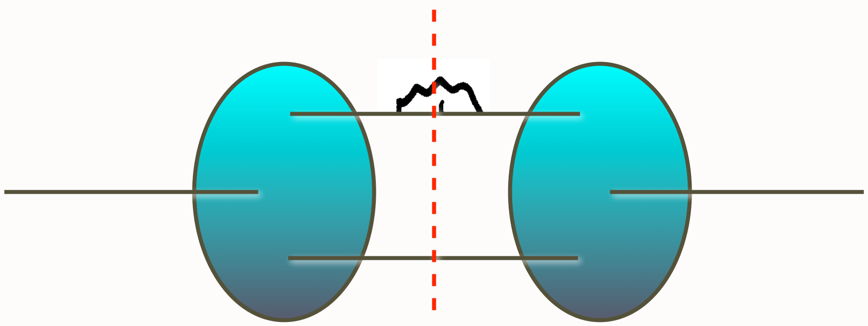

Lamb Shift n=3

$e^+e^-\gamma$

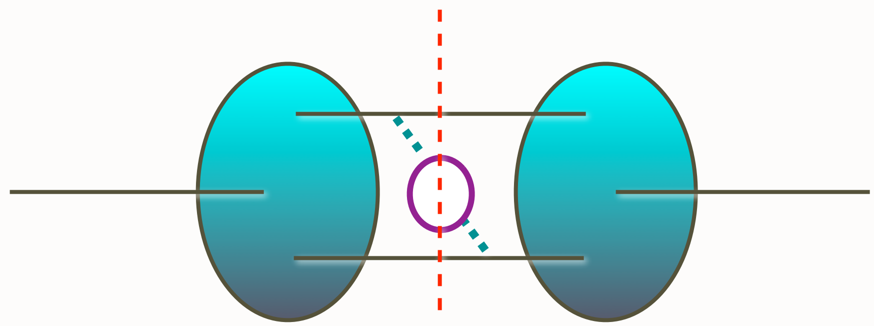

Vacuum Polarization n=4

$e^+e^-e^+e^-$

$$|p, S_z> = \sum_{n=3} \Psi_n(x_i, \vec{k}_{\perp i}, \lambda_i) | n; \vec{k}_{\perp_i}, \lambda_i >$$

sum over states with n=3, 4, ...constituents

The Light Front Fock State Wavefunctions

$$\Psi_n(x_i, \vec{k}_{\perp i}, \lambda_i)$$

are boost invariant; they are independent of the hadron's energy and momentum P^μ.

The light-cone momentum fraction

$$x_i = \frac{k_i^+}{p^+} = \frac{k_i^0 + k_i^z}{P^0 + P^z}$$

are boost invariant.

$$\sum_i^n k_i^+ = P^+, \ \sum_i^n x_i = 1, \ \sum_i^n \vec{k}_i^\perp = \vec{0}^\perp.$$

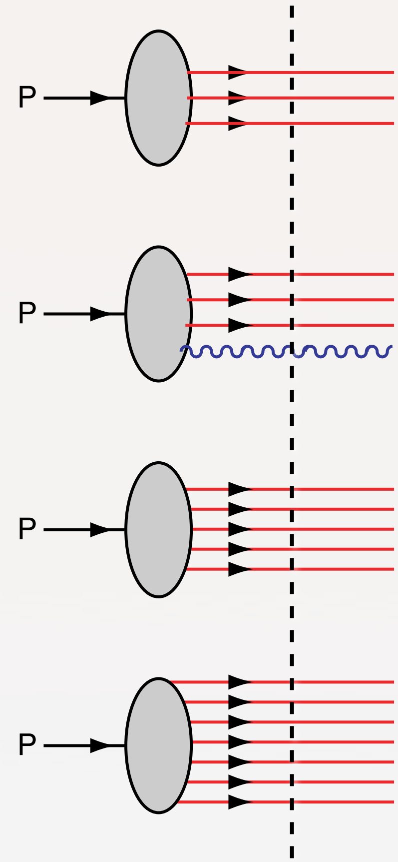

Fixed LF time

Intrinsic heavy quarks

$c(x), b(x)$ at high x

$\bar{s}(x) \neq s(x)$

$\bar{u}(x) \neq \bar{d}(x)$

Light-Front Wavefunctions: rigorous representation of composite systems in quantum field theory

Fixed $\tau = t + z/c$

$P^+ = P^0 + P^z$

$P^+, \vec{P}_\perp$

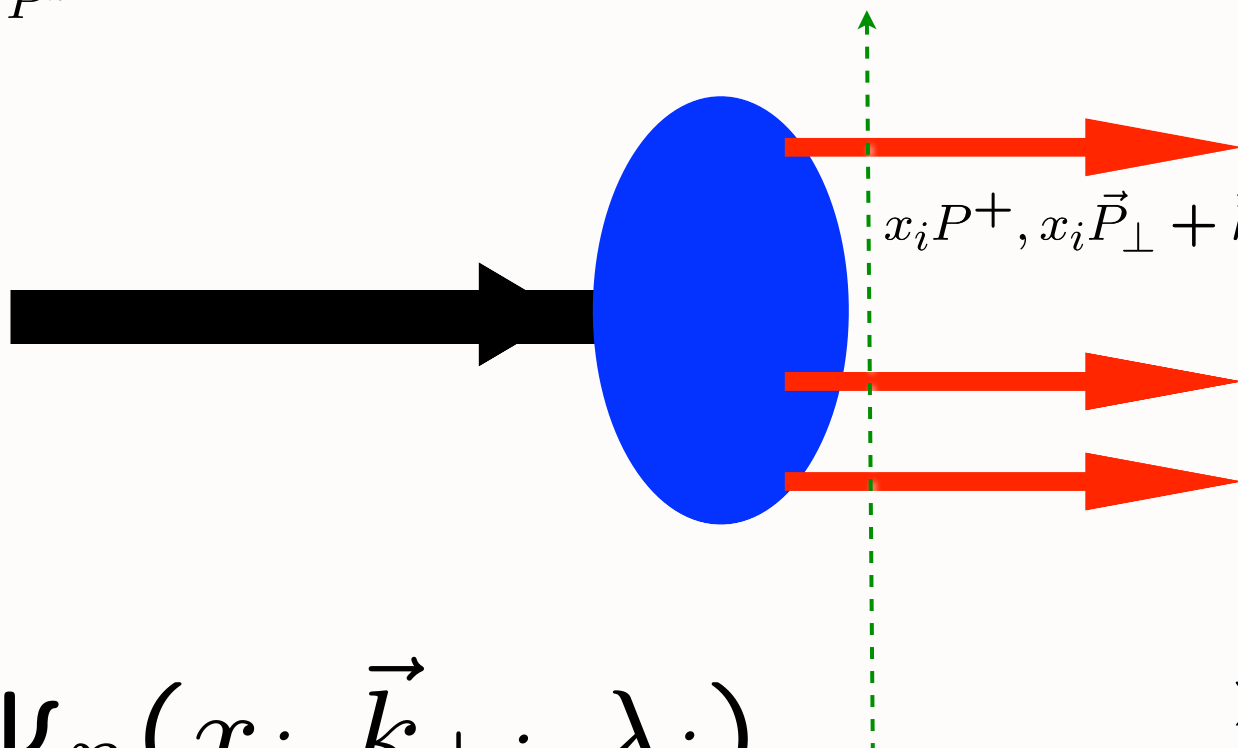

$x_i P^+, x_i \vec{P}_\perp + \vec{k}_{\perp i}$

$$\Psi_n(x_i, \vec{k}_{\perp i}, \lambda_i)$$

$\sum_i^n x_i = 1$

$\sum_i^n \vec{k}_{\perp i} = \vec{0}_\perp$

Invariant under boosts! Independent of P^μ

Diffractive Dissociation of Pion into Quark Jets

E791 Ashery et al.

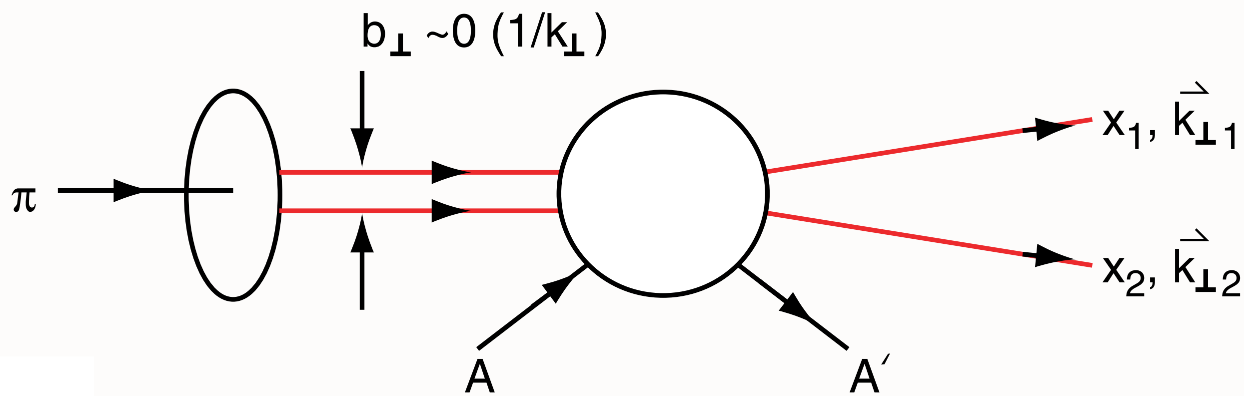

$$M \propto \frac{\partial^2}{\partial^2 k_\perp} \psi_\pi(x, k_\perp)$$

Measure Light-Front Wavefunction of Pion

Minimal momentum transfer to nucleus
Nucleus left Intact!

E791 FNAL Diffractive DiJet

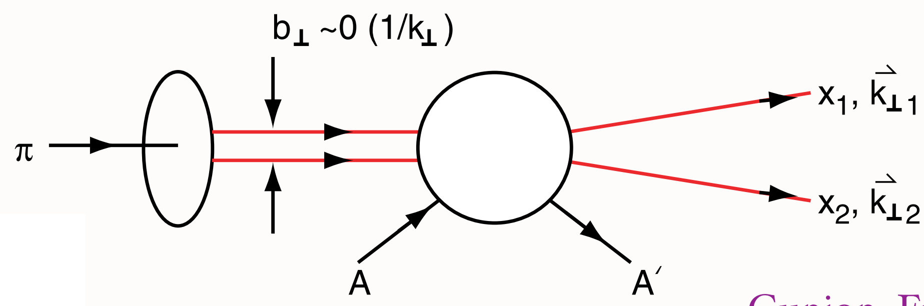

Gunion, Frankfurt, Mueller, Strikman, sjb
Frankfurt, Miller, Strikman

Two-gluon exchange measures the second derivative of the pion light-front wavefunction

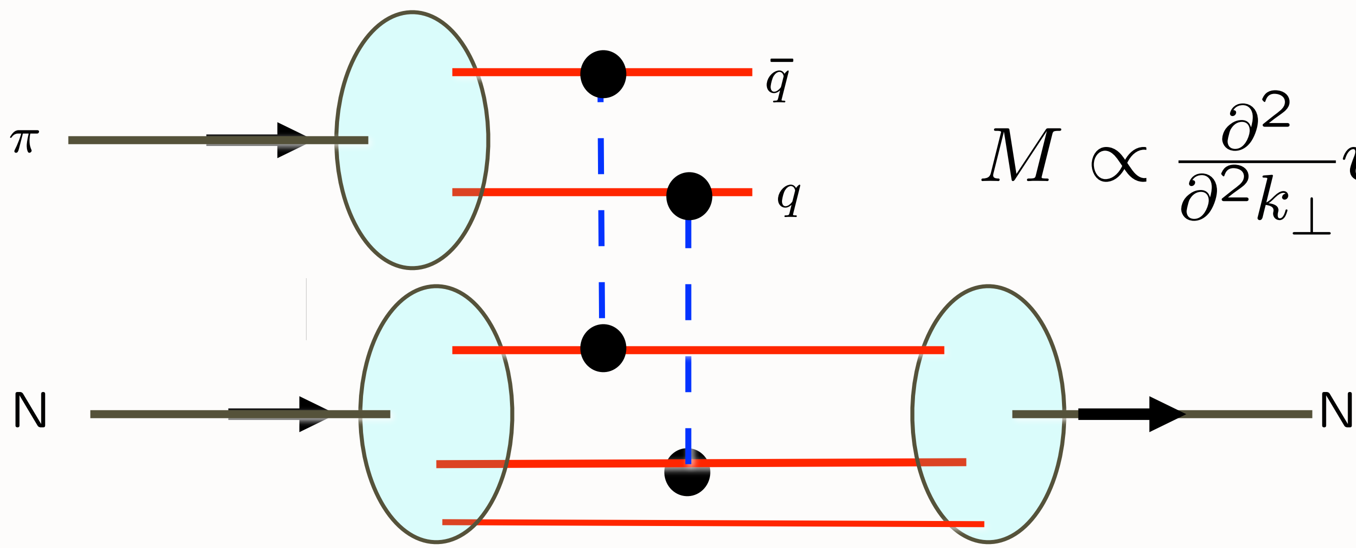

$$M \propto \frac{\partial^2}{\partial^2 k_\perp} \psi_\pi(x, k_\perp)$$

Diffractive Dissociation of Atoms

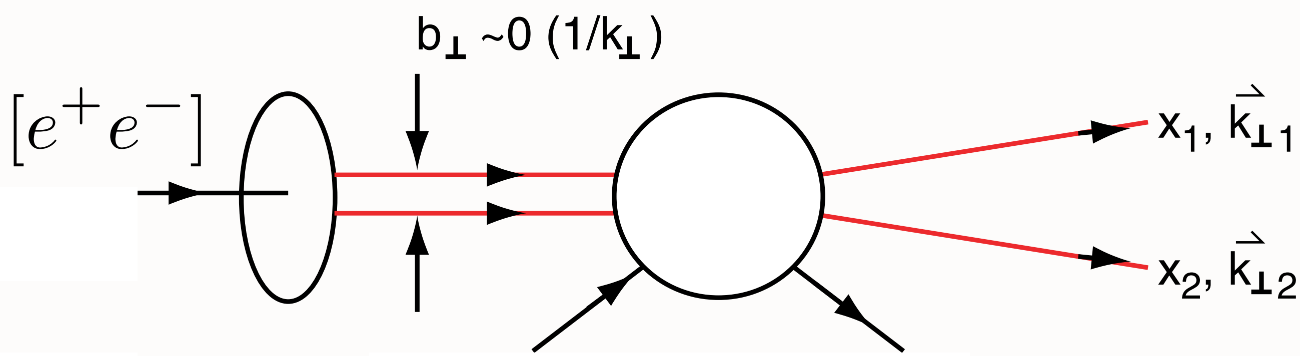

$$M \propto \frac{\partial}{\partial \vec{k}_\perp} \psi_{e^+e^-}(x, \vec{k}_\perp)$$

Measure Light-Front Wavefunction of Positronium and Other Atoms

Minimal momentum transfer to Target

Target left Intact!

- Fully coherent interactions between pion and nucleons.

- Emerging Di-Jets do not interact with nucleus.

$$\mathcal{M}(\mathcal{A}) = \mathcal{A} \cdot \mathcal{M}(\mathcal{N})$$

$$\underline{\frac{d\sigma}{dq_t^2} \propto A^2 \quad q_t^2 \sim 0}$$

$$\underline{\sigma \propto A^{4/3}}$$

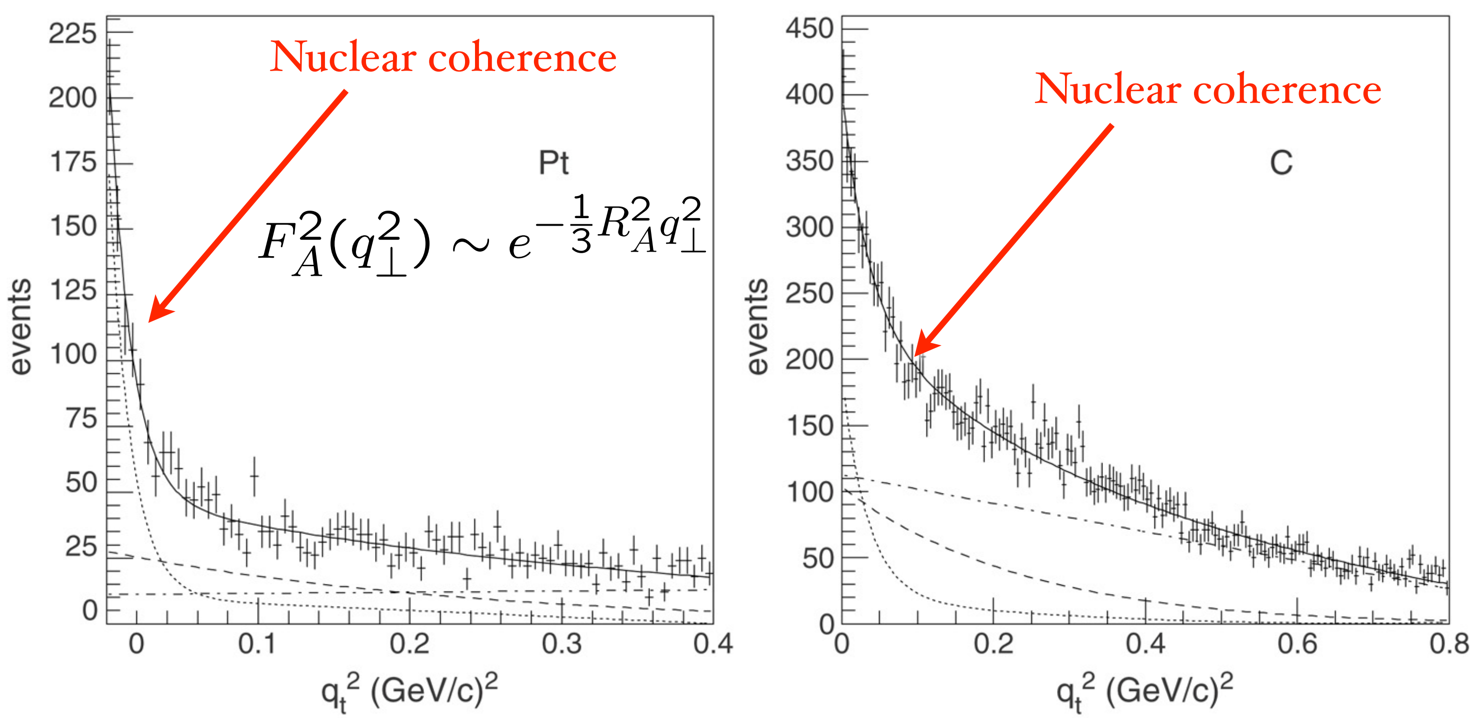

Mueller, sjb; Bertsch et al;
Frankfurt, Miller, Strikman

Measure pion LFWF in diffractive dijet production
Confirmation of color transparency

A-Dependence results: $\sigma \propto A^{\alpha}$

$\mathbf{k}_t$ range (GeV/c)	α	α (CT)
$1.25 < k_t < 1.5$	1.64 +0.06 -0.12	1.25
$1.5 < k_t < 2.0$	1.52 ± 0.12	1.45
$2.0 < k_t < 2.5$	1.55 ± 0.16	1.60

Ashery E791

α (Incoh.) $= 0.70 \pm 0.1$

Conventional Glauber Theory Ruled Out !

Factor of 7

Key Ingredients in E791 Experiment

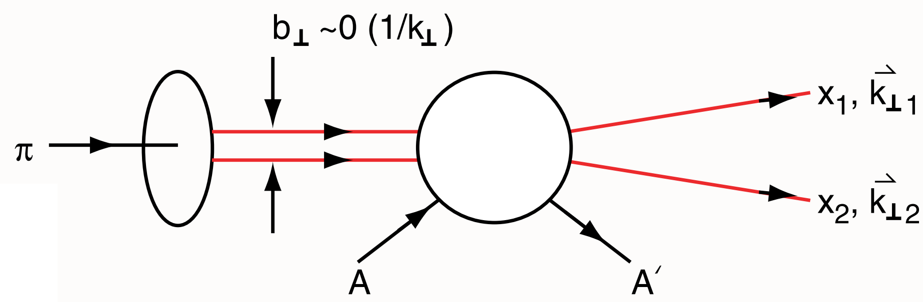

Brodsky Mueller
Frankfurt Miller Strikman

Small color-dipole moment pion not absorbed;
interacts with each nucleon coherently
QCD COLOR Transparency

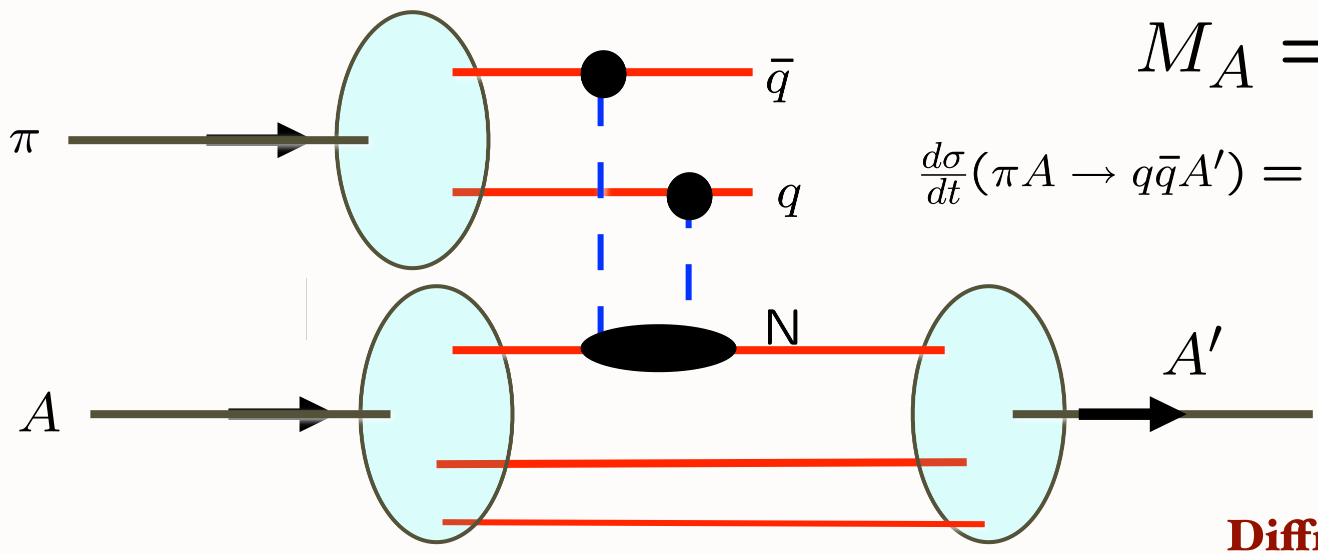

$$M_A = A\ M_N$$

$$\frac{d\sigma}{dt}(\pi A \to q\bar{q}A') = A^2\ \frac{d\sigma}{dt}(\pi N \to q\bar{q}N')\ F_A^2(t)$$

Target left intact

Diffraction, Rapidity gap

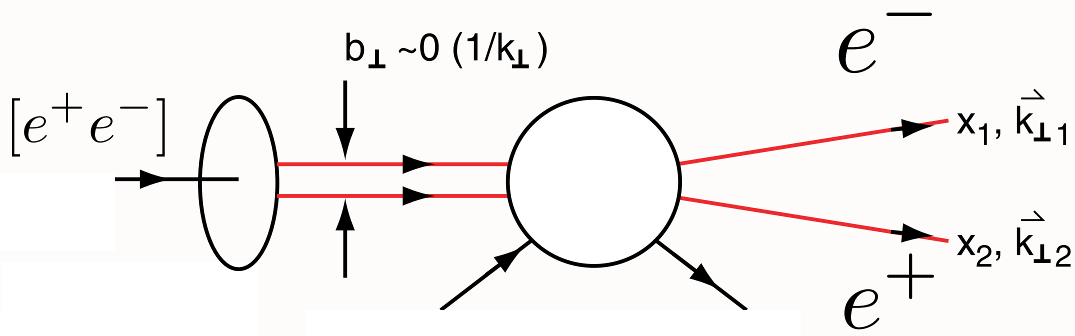

Coulomb-Photon exchange measures the derivative of the positronium light-front wavefunction

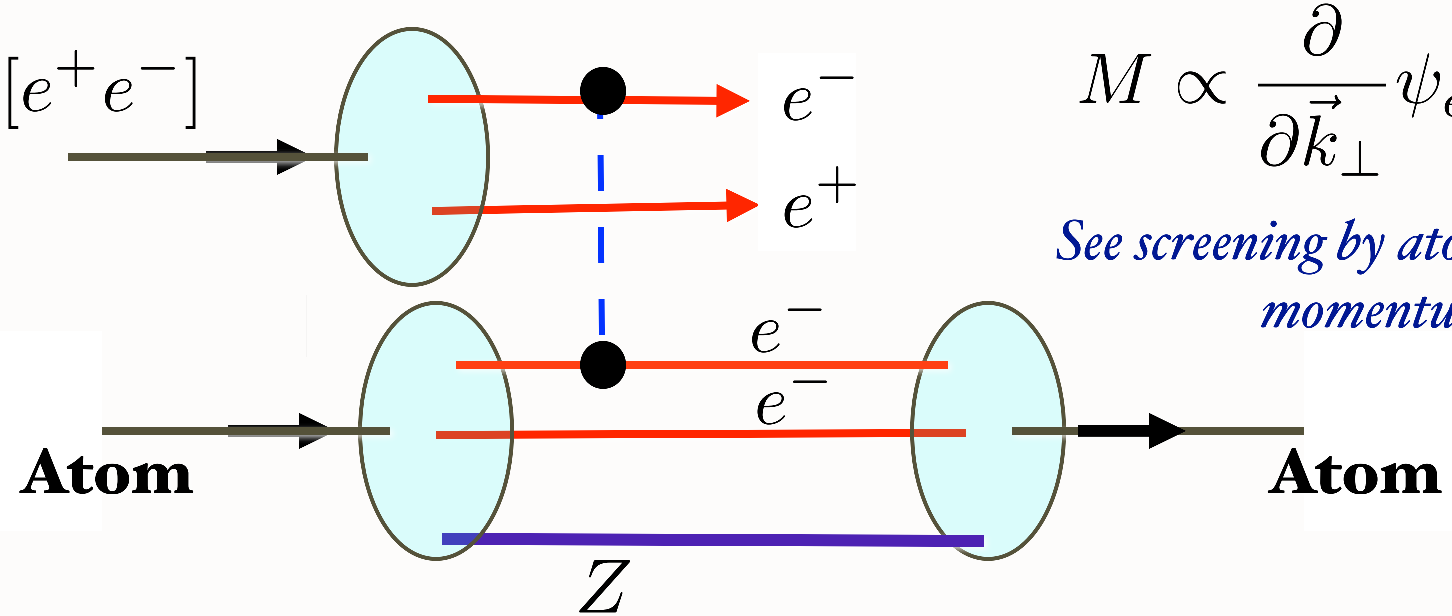

$$M \propto \frac{\partial}{\partial \vec{k}_\perp} \psi_{e^+e^-}(x, \vec{k}_\perp)$$

See screening by atomic electrons at low momentum transfer

Color Transparency

A. H. Mueller, sjb

Bertsch, Gunion, Goldhaber, sjb

- Fundamental test of gauge theory in hadron physics
- Small color dipole moments interact weakly in nuclei
- Complete coherence at high energies
- Clear Demonstration of CT from Diffractive Di-Jets

Atomic Transparency

- Fundamental test of gauge theory in atomic physics
- Small electric dipole moments interact weakly in target
- Complete coherence at high energies -- crystals!

E791 Diffractive Di-Jet transverse momentum distribution

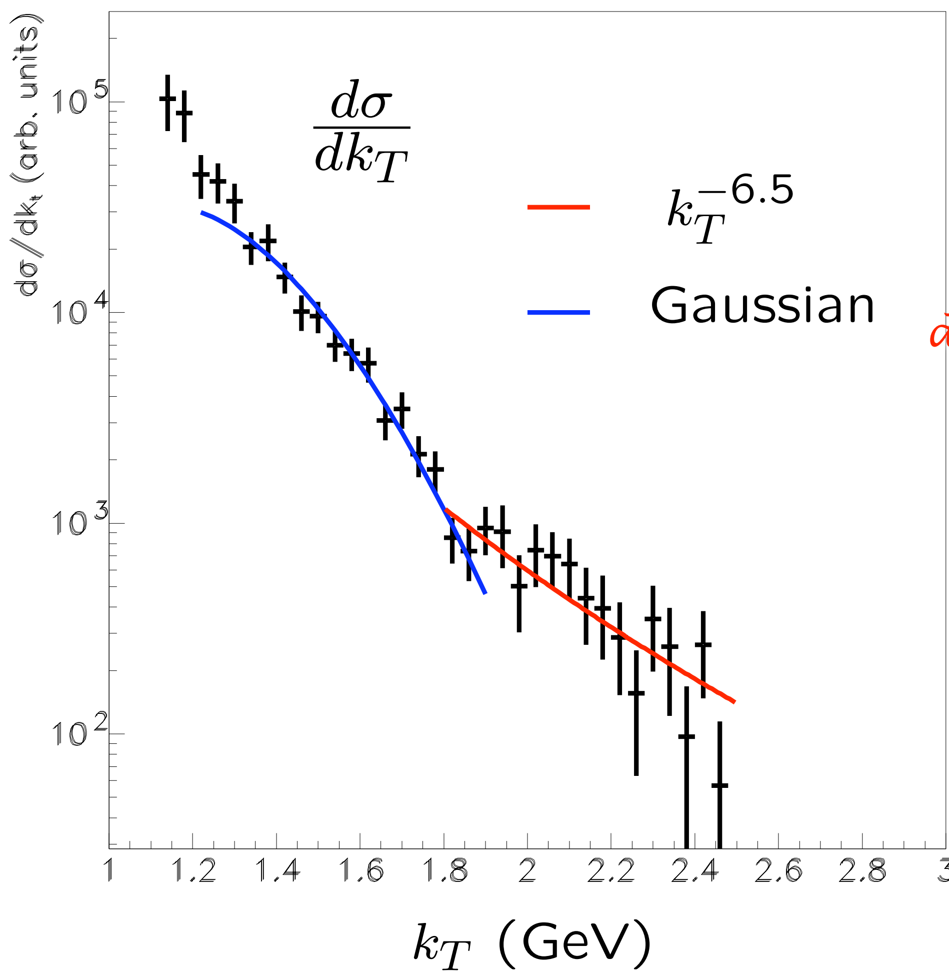

Two Components

High Transverse momentum dependence consistent with PQCD, ERBL Evolution $k_T^{-6.5}$

Gaussian component similar to AdS/CFT HO LFWF

Simulated diffractive transverse momentum distribution for positronium

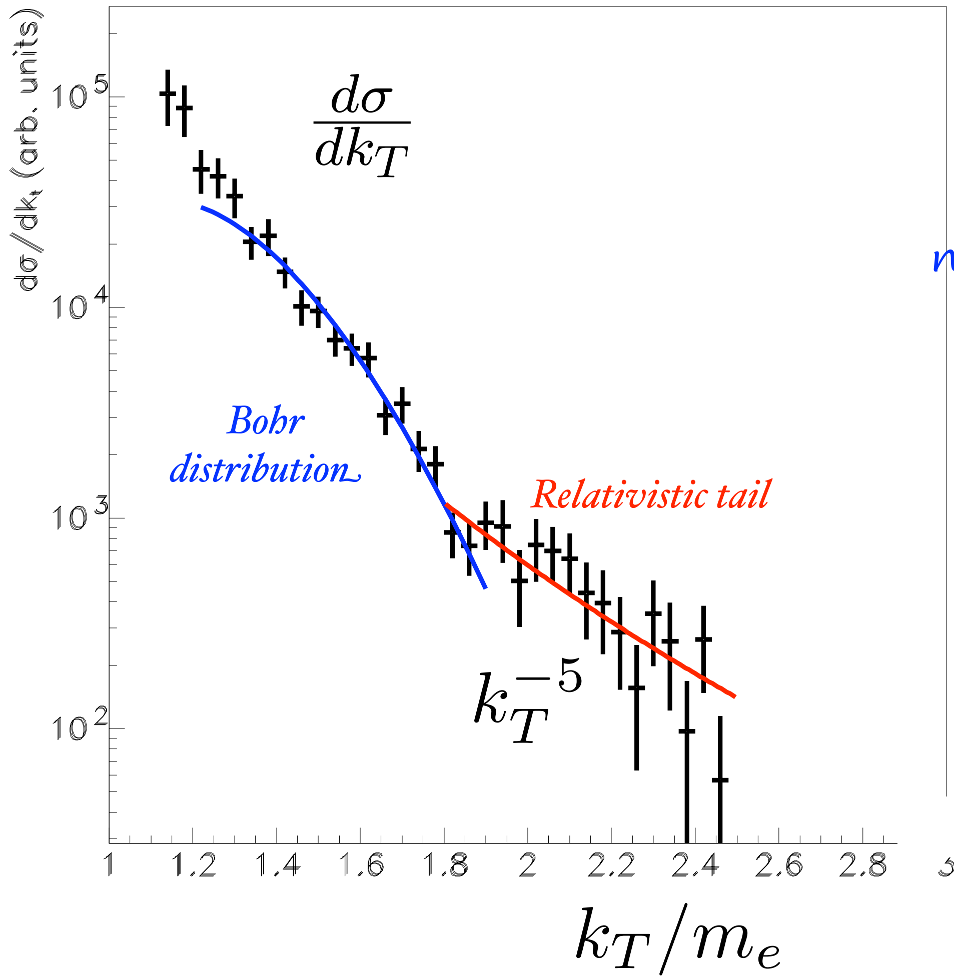

Two Components:

Low momentum dependence from non-relativistic Coulomb interaction

High Transverse momentum dependence from relativistic QED

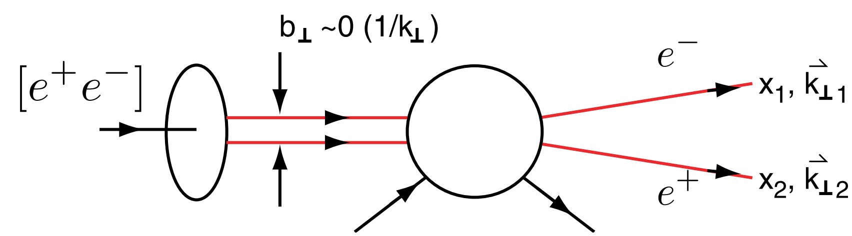

Positronium LFWF

G.P. Lepage, sjb

$$\left(M^2 - \frac{k_\perp{}^2 + m_1{}^2}{x_1} - \frac{k_\perp{}^2 + m_2{}^2}{x_2}\right)\psi(x_i, k_\perp) = \int_0^1 [dy] \int_0^\infty \frac{d^2 l_\perp}{16\pi^3} \tilde{K}(x_i, k_\perp; y_i, l_\perp; M^2)\psi(y_i, l_\perp)$$

$$\tilde{K} \simeq \frac{-16e^2 m^2}{(k_\perp - l_\perp)^2 + (x-y)^2 m^2}$$

Non-relativistic limit

$$\Psi = \left(\frac{m\beta^3}{\pi}\right)^{1/2} \frac{64\pi\beta x_1 x_2}{[k_\perp{}^2 + (x_1 - x_2)^2 m^2 + \beta^2]^2} \times \begin{cases} \dfrac{u_\uparrow \bar{v}_\downarrow - u_\downarrow \bar{v}_\uparrow}{(2x_1x_2)^{1/2}}, & \text{parapositronium}, \\ \dfrac{u_\uparrow \bar{v}_\uparrow}{(x_1x_2)^{1/2}}, & \text{orthopositronium}, \\ \cdots, & \end{cases}$$

$$\psi_{NR}(x, k_\perp) \sim \frac{1}{k_\perp^4}$$

$$\beta = \alpha m_e/2$$

At large $k_\perp^2 >> m_e^2$, $\psi(x, k_\perp) \sim \frac{1}{k_\perp^2}$

QCD Lagrangian

$$L_{QCD} = \overbrace{-\frac{1}{4g^2}\,\mathrm{Tr}(G^{\mu\nu}G_{\mu\nu})}^{\text{gluon dynamics}} + \overbrace{\sum_{f=1}^{nf} i\,\overline{\psi_f}\, D_\mu \gamma^\mu \psi_f}^{\text{quark kinetic energy + quark-gluon dynamics}} + \overbrace{\sum_{f=1}^{nf} m_f\, \overline{\psi_f}\, \psi_f}^{\text{mass term}}$$

QCD color charge field strength tensor covariant derivative quark field

$$\lim N_C \to 0 \text{ at fixed } \alpha = C_F \alpha_s, n_\ell = n_F / C_F$$

Analytic limit of QCD: Abelian Gauge Theory

QCD $\longrightarrow$ QED P. Huet, sjb

Huet, sjb

$$\lim N_C \to 0 \text{ at fixed } \alpha = C_F \alpha_s, n_\ell = n_F/C_F$$

$$\text{QCD} \to \text{Abelian Gauge Theory}$$

Analytic Feature of SU(Nc) Gauge Theory

All analyses for Quantum Chromodynamics must be applicable to Quantum Electrodynamics

Bethe-Maximon All-Orders Formula for Pair Production

PHYSICAL REVIEW VOLUME 93, NUMBER 4 FEBRUARY 15, 1954

Theory of Bremsstrahlung and Pair Production. I. Differential Cross Section

H. A. BETHE AND L. C. MAXIMON*
Laboratory of Nuclear Studies, Cornell University, Ithaca, New York
(Received October 29, 1953)

PHYSICAL REVIEW VOLUME 93, NUMBER 4 FEBRUARY 15, 1954

Theory of Bremsstrahlung and Pair Production. II. Integral Cross Section for Pair Production

HANDEL DAVIES,* H. A. BETHE, AND L. C. MAXIMON†
Laboratory of Nuclear Studies, Cornell University, Ithaca, New York
(Received October 29, 1953)

Bethe-Maximon All-Orders Formula for Pair Production

$$\gamma Z \to \ell^+ \ell^- Z$$

$$\sigma = 2a^2 \frac{e^2}{\hbar c}\left(\frac{\hbar}{mc}\right)^2 \frac{d\epsilon_1}{k^3}\left(\epsilon_1{}^2+\epsilon_2{}^2+\tfrac{2}{3}\epsilon_1\epsilon_2\right)$$

$$\times\left[2\log\frac{2\epsilon_1\epsilon_2}{k}-1-2f(Z)\right],$$

where

$$f(Z) = a^2 \sum_1^\infty \frac{1}{\nu(\nu^2+a^2)}.$$

$$\sum = (1+a^2)^{-1}+0.20206-0.0369a^2$$
$$+0.0083a^4-0.002a^6.$$

$$a = Z\alpha$$

• Lepton Charge Asymmetry

PHYSICAL REVIEW VOLUME 173, NUMBER 4 20 SEPTEMBER 1968

Second Born Corrections to Wide-Angle High-Energy Electron Pair Production and Bremsstrahlung*

STANLEY J. BRODSKY
Stanford Linear Accelerator Center, Stanford University, Stanford, California 94305

AND

JOHN R. GILLESPIE
Centre de Physique Théorique, Ecole Polytechnique,† Paris, France and Stanford Linear Accelerator Center, Stanford University, Stanford, California 94305

(Received 15 April 1968)

$$\gamma Z \rightarrow \ell^+ \ell^- Z$$

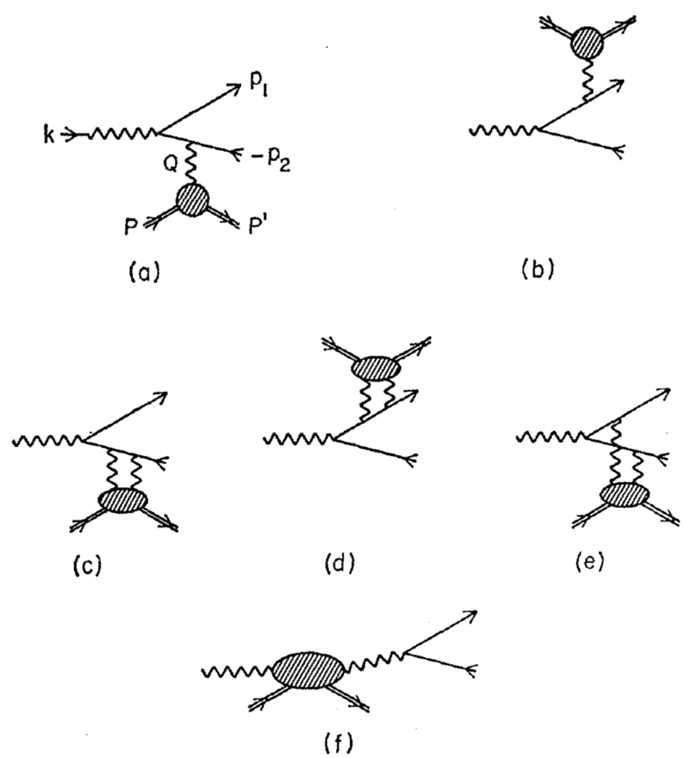

• Lepton Charge Asymmetry

$$\gamma Z \to \ell^+ \ell^- Z$$

$$\epsilon(\delta) = \frac{N_+(\delta) - N_-(\delta)}{N_+(\delta) + N_-(\delta)}$$

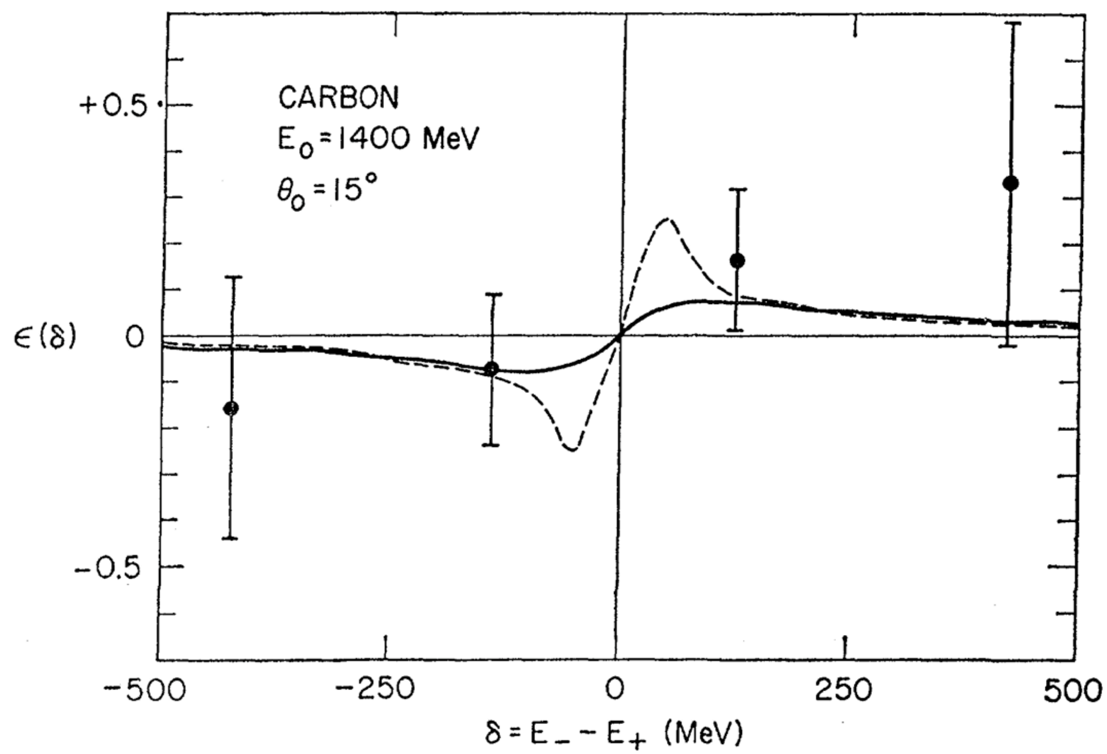

Electron-positron asymmetry in pair production on carbon for invariant pair mass $m(e^+e^-) = 770 \pm 50$ MeV (the ρ^0-dominated region). The definition of $\epsilon(\delta)$ is given in Sec. I. The experimental points are the binned results of Ref. 7. The dashed curve is the second Born spin-zero result given in Sec. IV for mirror-symmetric (except for energy, $\delta = E_1 - E_2$) pairs produced in a Yukawa charge distribution, with $\mu = 204$ MeV chosen to fit the carbon rms radius. The solid curve is obtained by averaging the cross sections over lepton angles in order to approximate the experimental acceptance, as discussed in the text.

• *Lepton Charge Asymmetry*

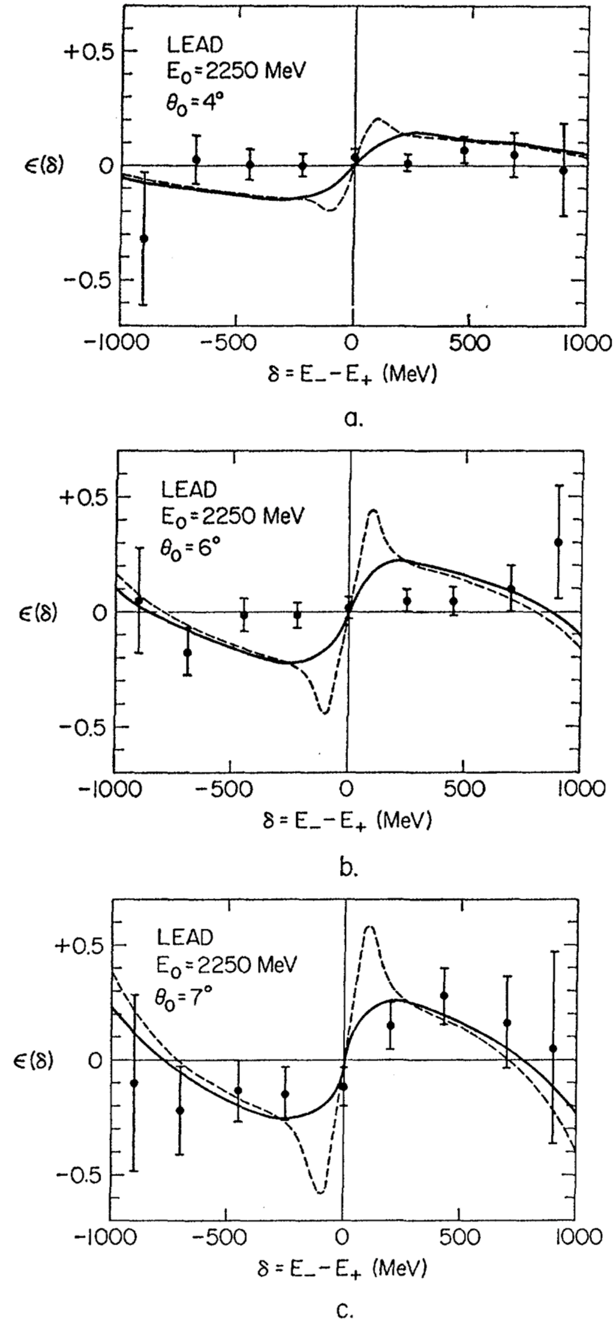

Electron-positron asymmetry in pair production on lead for invariant pair mass in the interval $300 \leq m(e^+e^-) \leq 550$ MeV. The experimental points are from Ref. 7. The dotted curve is the predicted differential cross section for mirror-symmetric (except for $E_- - E_+ = \delta$) pairs produced in a Yukawa charge distribution, with $\mu = 89.5$ MeV chosen to fit the electromagnetic rms radius of lead. The solid curve is obtained from an average over lepton angles to provide a first approximation to the experimental acceptance (see text). The asymmetry for $|\delta| \leq 300$ MeV will be reduced when the theoretical prediction is averaged over the finite binning size and the actual experimental acceptance.

$$\frac{d\sigma_- - d\sigma_+}{d\sigma_+ + d\sigma_+} = \frac{\pi Z \alpha \sin\theta/2}{1 + \sin\theta/2}$$

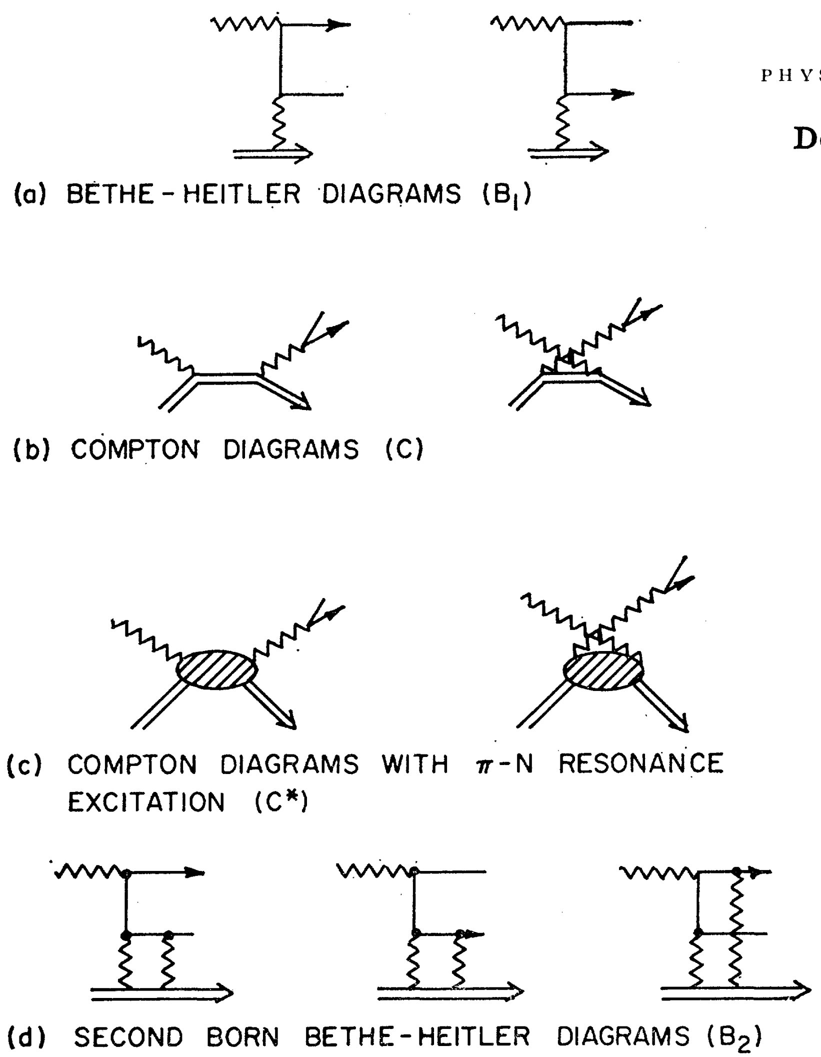

PHYSICAL REVIEW VOLUME 187, NUMBER 5 25 NOVEMBER 196

Determination of the Real Part of the Compton Amplitude at a Nucleon Resonance*

STANLEY J. BRODSKY
Stanford Linear Accelerator Center, Stanford University, Stanford, California 94305

AND

ANTHONY C. HEARN†
Institute of Theoretical Physics, Department of Physics, Stanford University, Stanford, California 94305

AND

RONALD G. PARSONS
Center for Particle Theory, Department of Physics, The University of Texas, Austin, Texas 78712

(Received 28 July 1969)

The real part of the virtual Compton amplitude can be directly determined from measurements of electron (or muon) bremsstrahlung or pair photoproduction. In general, the interference of the Compton amplitude with the Bethe-Heitler amplitude for pair production or bremsstrahlung yields a contribution to the cross section which is antisymmetric when the leptons are interchanged. This interference contribution thus produces different cross sections for electron and positron bremsstrahlung at a given scattering energy and angle. Also, the counting rate for pair production will depend on which lepton has the greater momentum. The determination of the real part of the Compton amplitude would supply information on the isobar resonance shape, test the dispersion relation for the forward amplitude, and resolve uncertainties in the determination of the nucleon resonances. A simple estimate for the lepton asymmetry of the pair production cross sections due to the forward Compton amplitude is given, in addition to a complete calculation of the effect of the first nucleon resonance using the isobar model. The results are also discussed for nuclear targets. For the latter case, a broadening of the isobar decay width due to absorption in the nuclear medium must be taken into account.

DVCS Physics

PHYSICAL REVIEW D

PARTICLES AND FIELDS

THIRD SERIES, VOL. 2, NO. 3 1 AUGUST 1970

Asymmetric Electron Pair Production on Carbon*†

R. M. SIMONDS‡
High Energy Physics Laboratory, Stanford University, Stanford, California 94305

AND

B. RICHTER
Stanford Linear Accelerator Center, Stanford, California 94305

(Received 13 April 1970)

The cross section for the reaction $\gamma + \mathrm{C} \rightarrow e^+ + e^- + \mathrm{C}$ has been measured for a series of kinematic point giving nuclear momentum transfers in the region 0.2–0.7 F^{-2}, with incident photon energies in the regio for photoproduction of the first two pion-nucleon resonances. Measurements were made, using asymmetri detection geometry, of electron and positron cross sections for each point. The charge-independent yield are shown to be in agreement with predictions of quantum electrodynamics for coherent and quasi-elasti production on carbon. The charge-asymmetric results are shown to be consistent with recent estimates of th interference between Bethe-Heitler and Compton pair production amplitudes with excitation of an inter mediate π-N state in the Compton diagram.

TABLE VII. Comparison of experimental and theoretical results.

E_0 (MeV)	$p_\pm$ (MeV/c)	θ (deg)	Polarity	Expt yield/V	Theor yield/V	$R_{(\mathrm{expt/theor})}$	A_{theor} Eq. (20)	A_{expt}	$A_{(\mathrm{expt/theor})}$
390	170	30.00	+	8.74±0.95	8.55	1.02±0.11	−0.041	−0.05 ±0.08	1.2 ±1.9
			−	7.90±0.96	8.24	0.96±0.12			
	340	18.10	+	3.24±0.22	3.36	0.96±0.07	0.052	0.21 ±0.05	4.0 ±1.0
			−	4.92±0.37	3.61	1.36±0.10			
550	450	14.85	+	6.36±0.44	6.84	0.93±0.06	0.096	0.063±0.053	0.66±0.55
			−	7.21±0.57	8.04	0.90±0.07			
		20.40	+	1.13±0.12	1.16	0.97±0.10	0.142	0.092±0.072	0.65±0.51
			−	1.36±0.13	1.41	0.96±0.09			
715	625	10.15	+	7.82±0.92	12.31	0.64±0.08	0.068	0.270±0.112	4.0 ±1.6
			−	13.59±2.2	14.02	0.97±0.16			
		13.00	+	2.91±0.28	3.28	0.89±0.09	0.099	0.041±0.068	0.41±0.69
			−	3.16±0.30	3.84	0.82±0.08			
		14.95	+	1.36±0.16	1.52	0.90±0.11	0.108	0.176±0.076	1.6 ±0.7
			−	1.94±0.19	1.80	1.08±0.11			

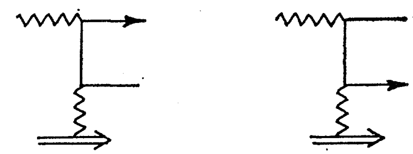

(a) BETHE-HEITLER DIAGRAMS (B_1)

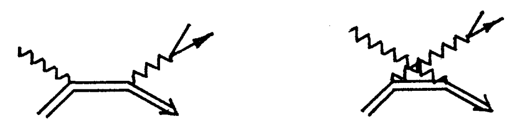

(b) COMPTON DIAGRAMS (C)

(c) COMPTON DIAGRAMS WITH π-N RESONANCE EXCITATION (C*)

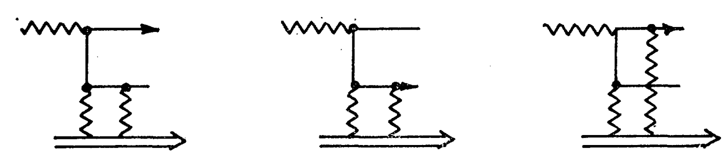

(d) SECOND BORN BETHE-HEITLER DIAGRAMS (B_2)

J=0 Fixed Pole Contribution to DVCS

- J=0 fixed pole -- direct test of QCD locality -- from seagull or instantaneous contribution to Feynman propagator

Szczepaniak, Llanes-Estrada, sjb

Close, Gunion, sjb

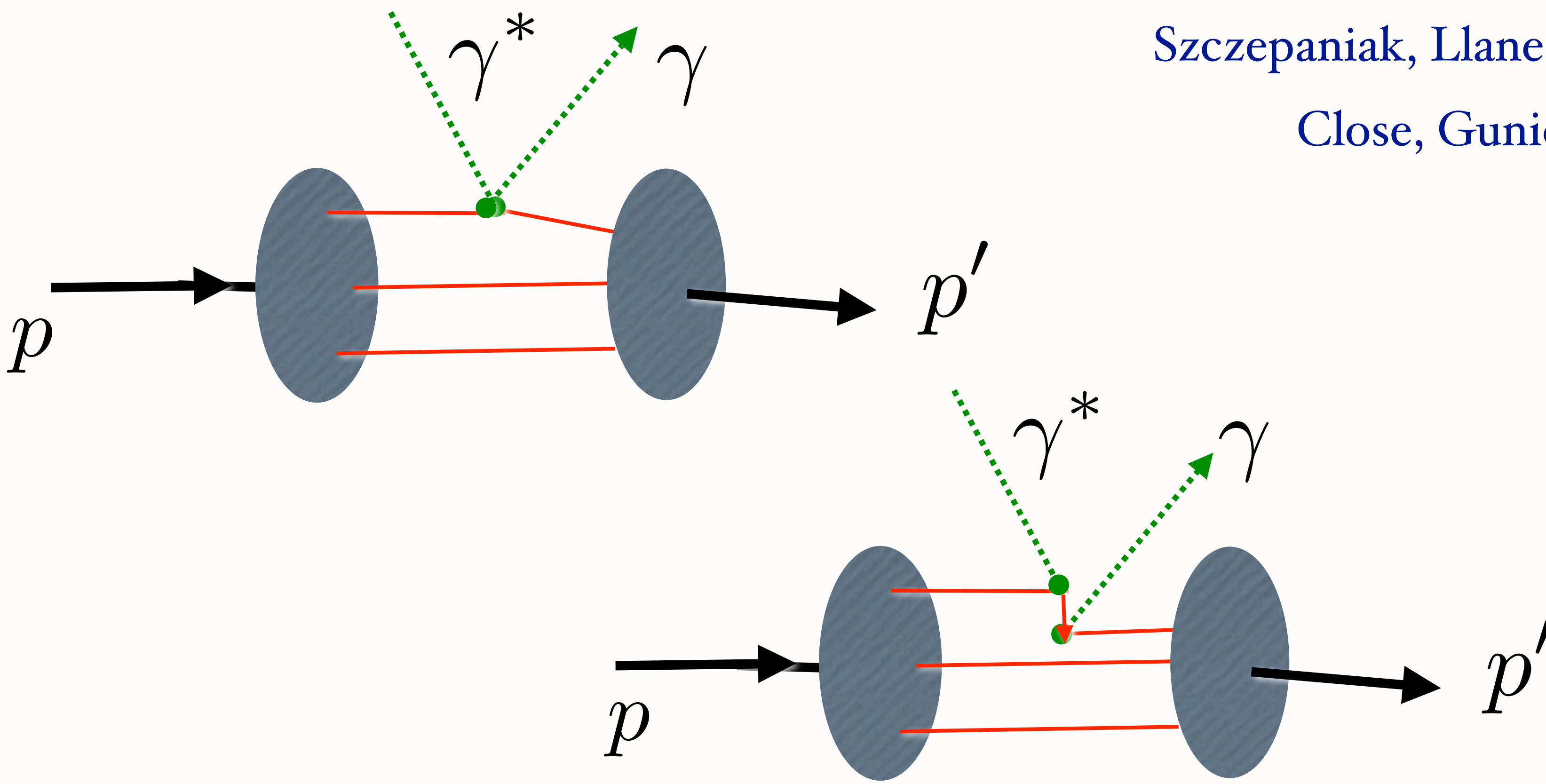

Real amplitude, independent of Q^2 at fixed t

Deeply Virtual Compton Scattering

$$\gamma^* p \to \gamma p$$

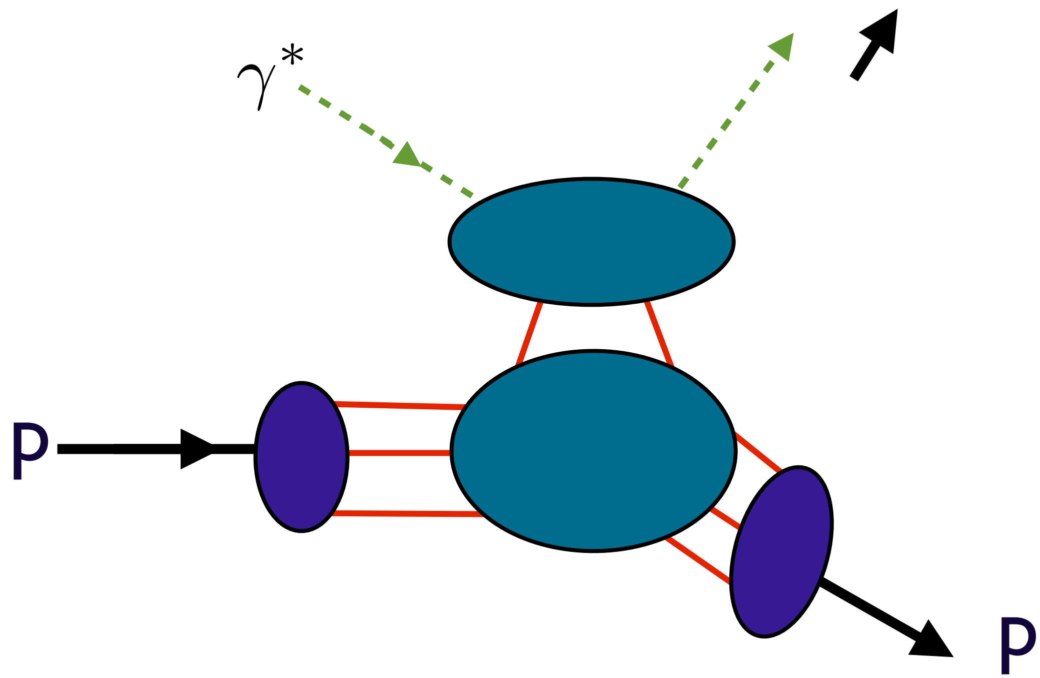

Hard Reggeon Domain

$$s >> -t, Q^2 >> \Lambda^2_{QCD}$$

$$T(\gamma^*(q)p \to \gamma(k) + p) \sim \epsilon \cdot \epsilon' \sum_R s^{\alpha}_R(t) \beta_R(t)$$

$$\alpha_R(t) \to 0$$

Reflects elementary coupling of two photons to quarks

$$\beta_R(t) \sim \frac{1}{t^2}$$

$$\frac{d\sigma}{dt} \sim \frac{1}{s^2} \frac{1}{t^4} \sim \frac{1}{s^6} \text{ at fixed } \frac{Q^2}{s}, \frac{t}{s}$$

Deeply Virtual Compton Scattering

$$\gamma^* p \to \gamma p$$

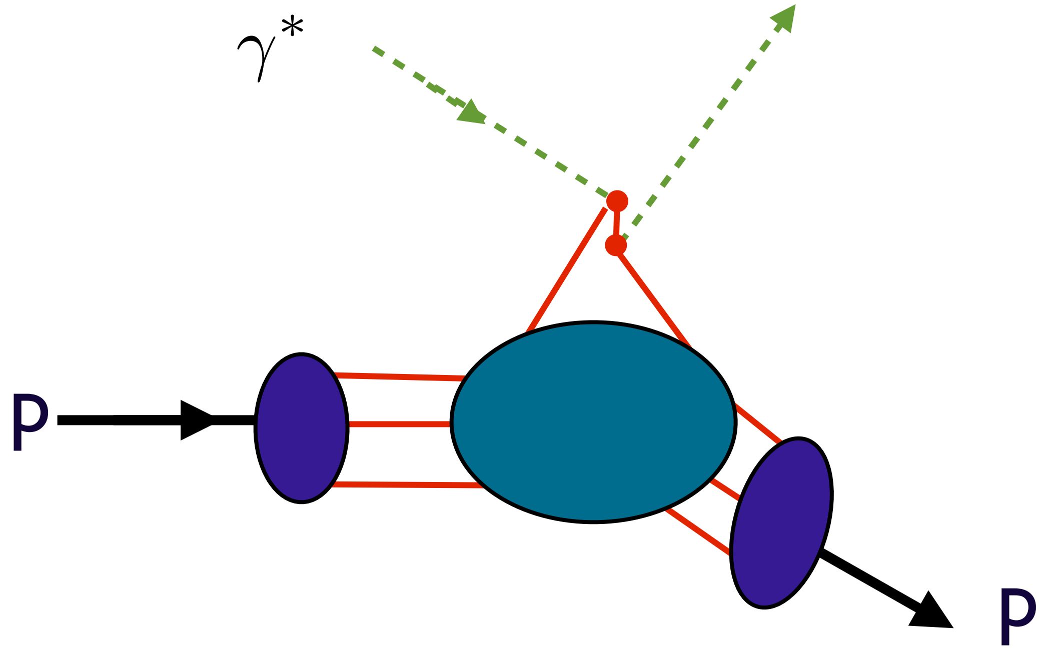

Seagull interaction (instantaneous quark exchange or Z-graph)

$$s >> -t, Q^2 >> \Lambda^2_{QCD}$$

Hard Reggeon Domain

$$T(\gamma^*(q)p \to \gamma(k) + p) \sim \epsilon \cdot \epsilon' \sum_R s_R^{\alpha}(t)\beta_R(t)$$

$$\alpha_R(t) \to 0$$

Reflects elementary coupling of two photons to quarks

$$\beta_R(t) \sim \frac{1}{t^2}$$

$$\frac{d\sigma}{dt} \sim \frac{1}{s^2}\frac{1}{t^4} \sim \frac{1}{s^6} \text{ at fixed } \frac{Q^2}{s}, \frac{t}{s}$$

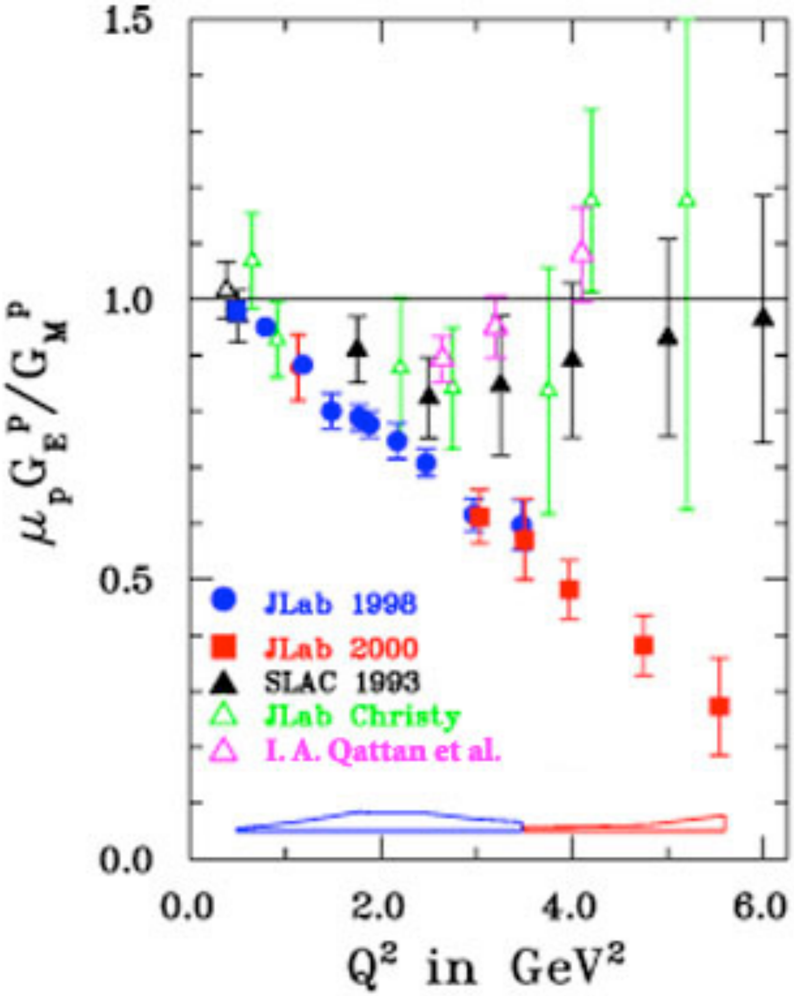

Figure 1: The ratios $\mu_p G_E{}^p / G_M{}^p$ from the two JLab recoil polarization experiments, compared to the Rosenbluth separation data.

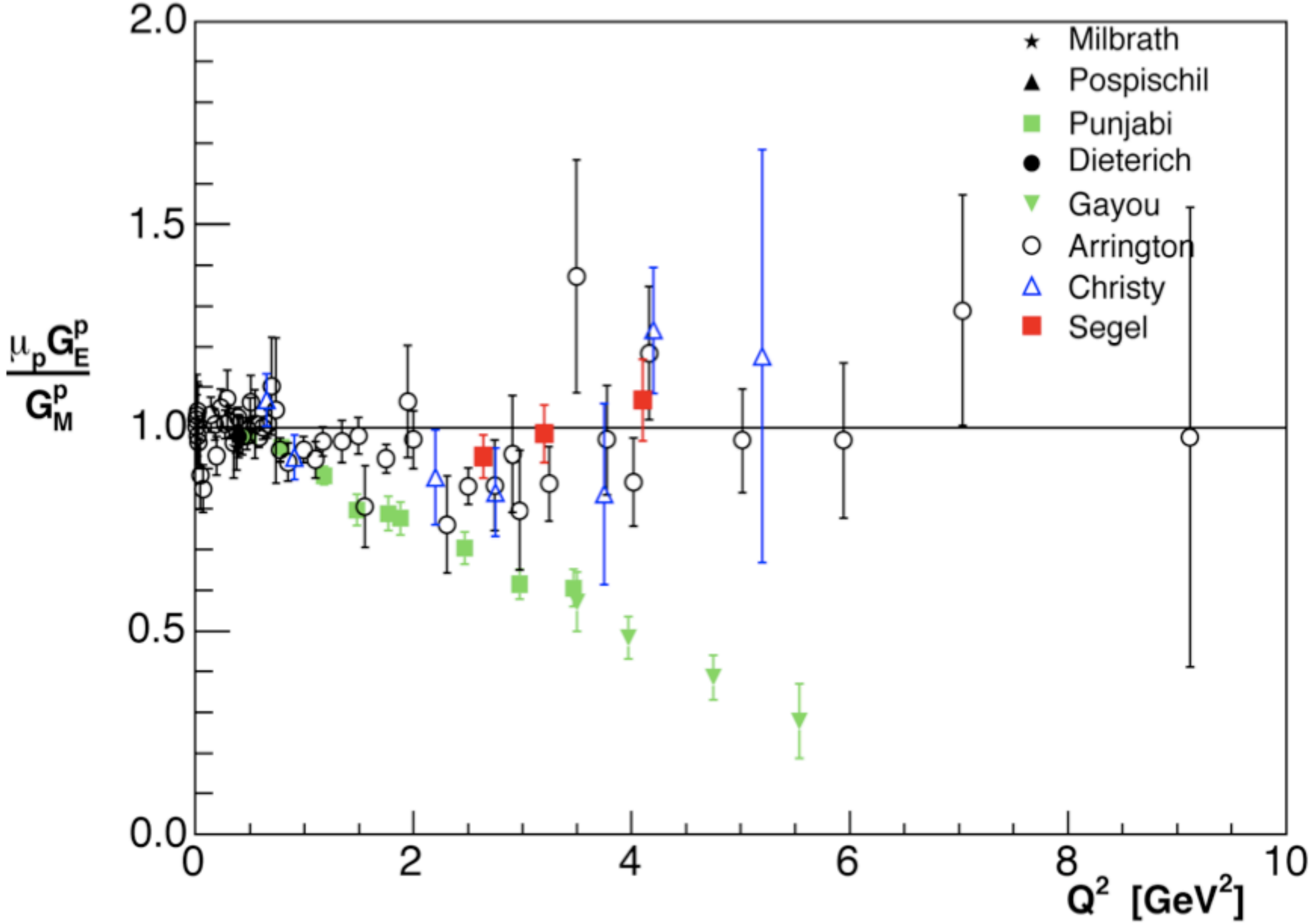

2.0
1.5
1.0
0.5
0.0
0
2
4
6
8
10
$\frac{\mu_p G_E^p}{G_M^p}$
Q^2 [GeV^2]
Milbrath
Pospischil
Punjabi
Dieterich
Gayou
Arrington
Christy
Segel

Breakdown of Rosenbluth Formula for G_E, G_M separation

- Two-photon exchange correction, elastic and inelastic nucleon channels significant; interference with one-photon exchange destroys Rosenbluth method

  Blunden, Melnitchouk; Afanasev, Chen,Carlson, Vanderhaegen, sjb

- Use J-Lab polarization transfer method

- Timelike form factors for radiative return; angular separation

- $e^+ e^-$ charge asymmetry from interference of 1 and 2 photon amplitudes

Test Landau-Pomeranchuk-Migdal (LPM) Effect

Physics Letters B 298 (1993) 165–170
North-Holland

PHYSICS LETTERS B

A bound on the energy loss of partons in nuclei ☆

Stanley J. Brodsky
Stanford Linear Accelerator Center, Stanford University, Stanford, CA 94309, USA

and

Paul Hoyer
Department of Physics, University of Helsinki, SF-00170 Helsinki, Finland

Received 17 October 1992

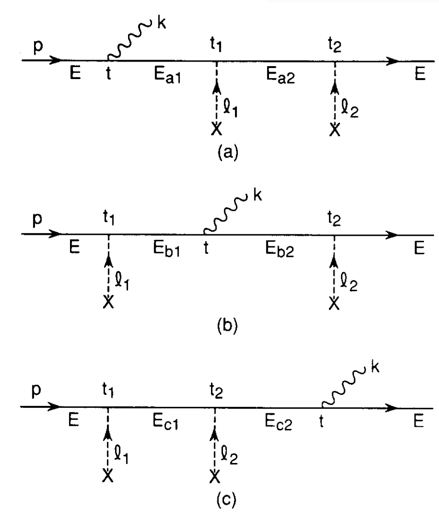

Multiple scattering can induce a fixed energy loss in the laboratory frame.

In general, the fractional energy loss x that can be induced by multiple scattering in a target of length L_A is limited by

$$\Delta x < \frac{\overline{k_\perp^2}\, L_A}{2E_{lab}}$$

Indirect Dark Matter Searches in the Light of ATIC, FERMI, EGRET and PAMELA

W. de Boer

Institut für Experimentelle Kernphysik
KIT, D-76131 Karlsruhe, Germany

arXiv:0910.2601

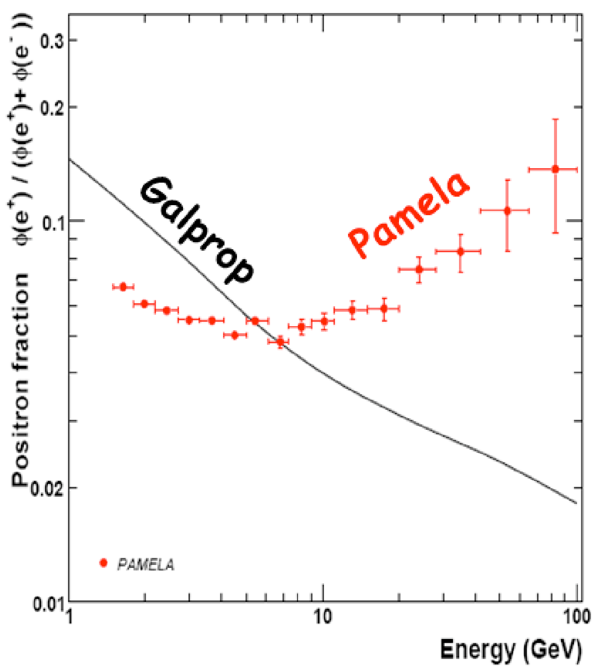

Positron fraction as measured by PAMELA in comparison with the GALPROP prediction.

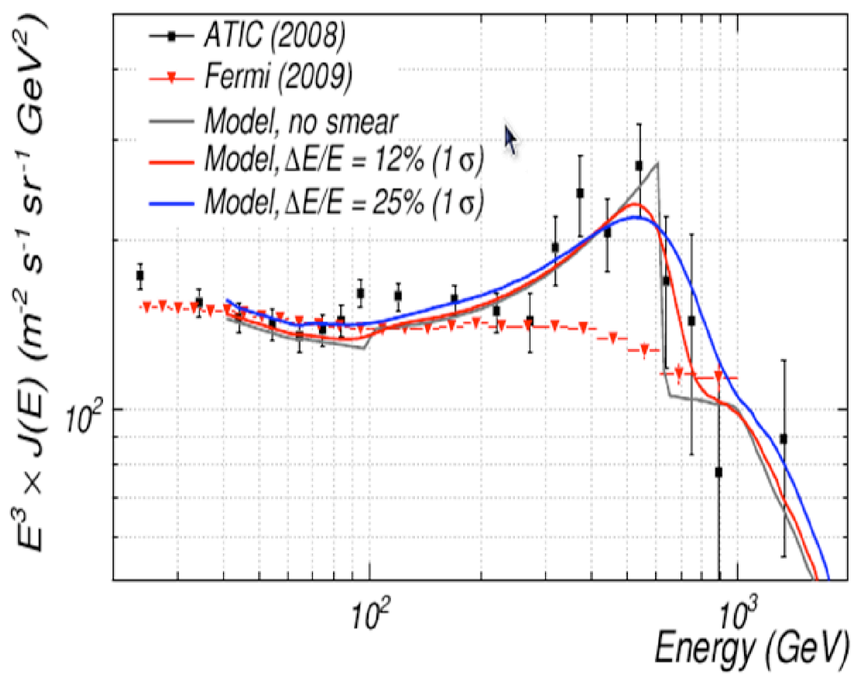

Spectrum of electrons+positrons from FERMI and ATIC.

Question: Has high x_F charm hadroproduction been modeled correctly?

Measurement of Charm Structure Function

J. J. Aubert et al. [European Muon Collaboration], “Production Of Charmed Particles In 250-Gev Mu+ - Iron Interactions,” Nucl. Phys. B 213, 31 (1983).

First Evidence for Intrinsic Charm

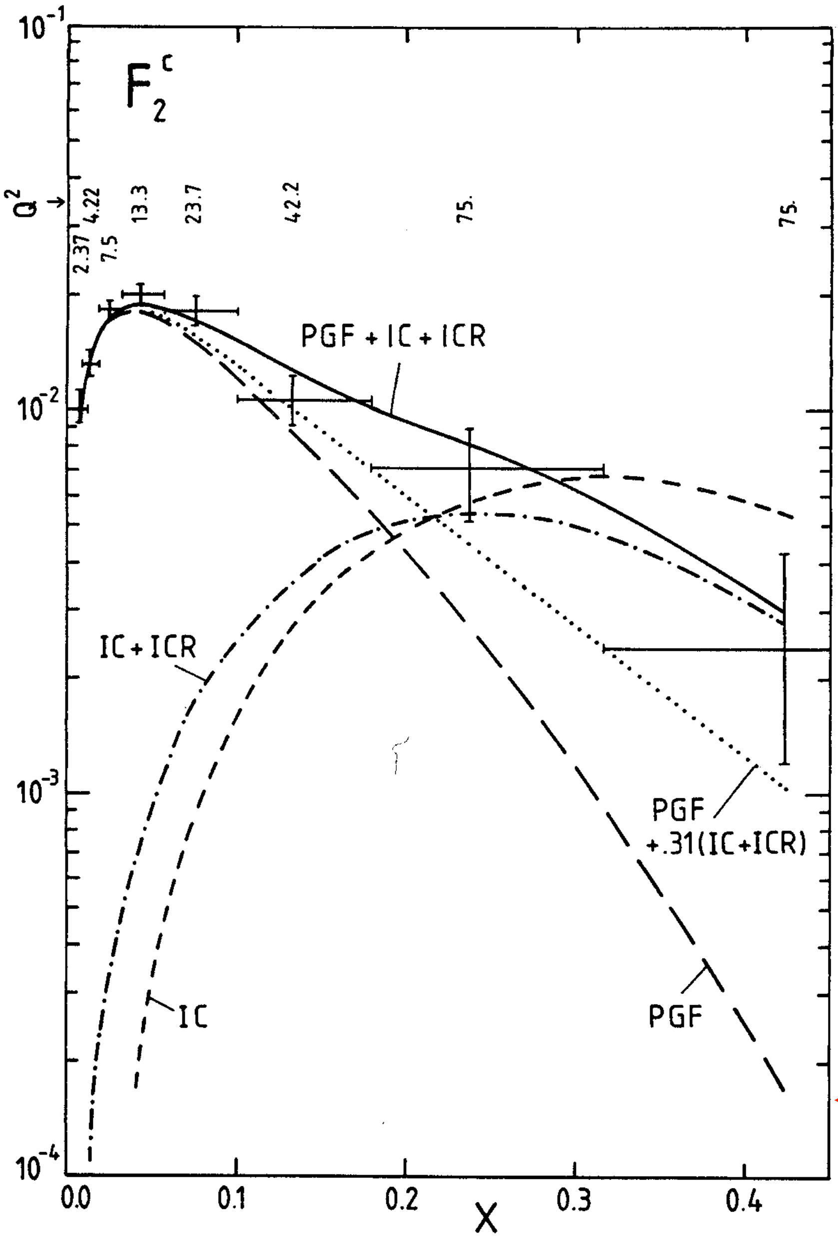

factor of 30 !

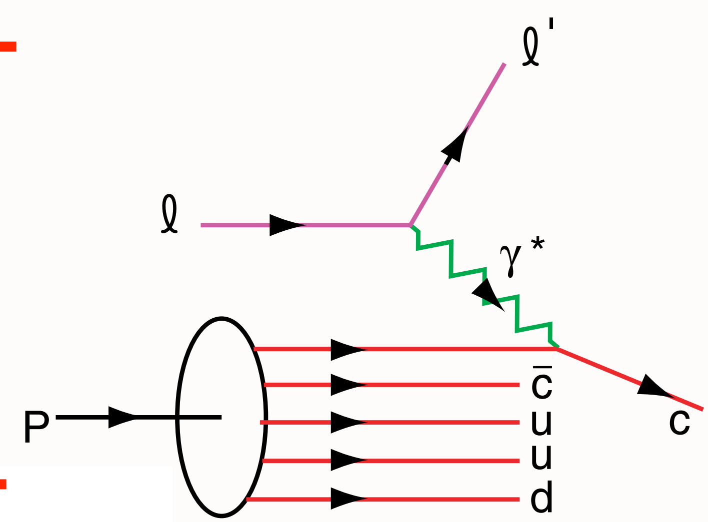

DGLAP / Photon-Gluon Fusion: factor of 30 too small

Intrinsic Heavy-Quark Fock States

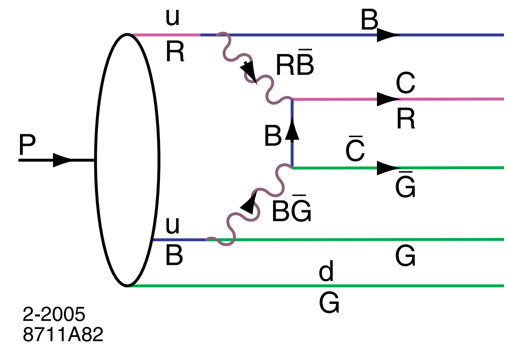

- Rigorous prediction of QCD, OPE
- Color-Octet Color-Octet Fock State!
- Probability $P_{Q\bar{Q}} \propto \frac{1}{M_Q^2}$ $\quad P_{Q\bar{Q}Q\bar{Q}} \sim \alpha_s^2 P_{Q\bar{Q}}$ $\quad P_{c\bar{c}/p} \simeq 1\%$
- Large Effect at high x

Collins, Ellis, Gunion, Mueller, sjb

- Greatly increases kinematics of colliders such as Higgs production (**Kopeliovich, Schmidt, Soffer, sjb**)
- Severely underestimated in conventional parameterizations of heavy quark distributions (**Pumplin, Tung**)
- Many empirical tests

PRL **102,** 192002 (2009) PHYSICAL REVIEW LETTERS week ending 15 MAY 2009

Measurement of $\gamma + b + X$ and $\gamma + c + X$ Production Cross Sections in $p\bar{p}$ Collisions at $\sqrt{s} = 1.96$ TeV

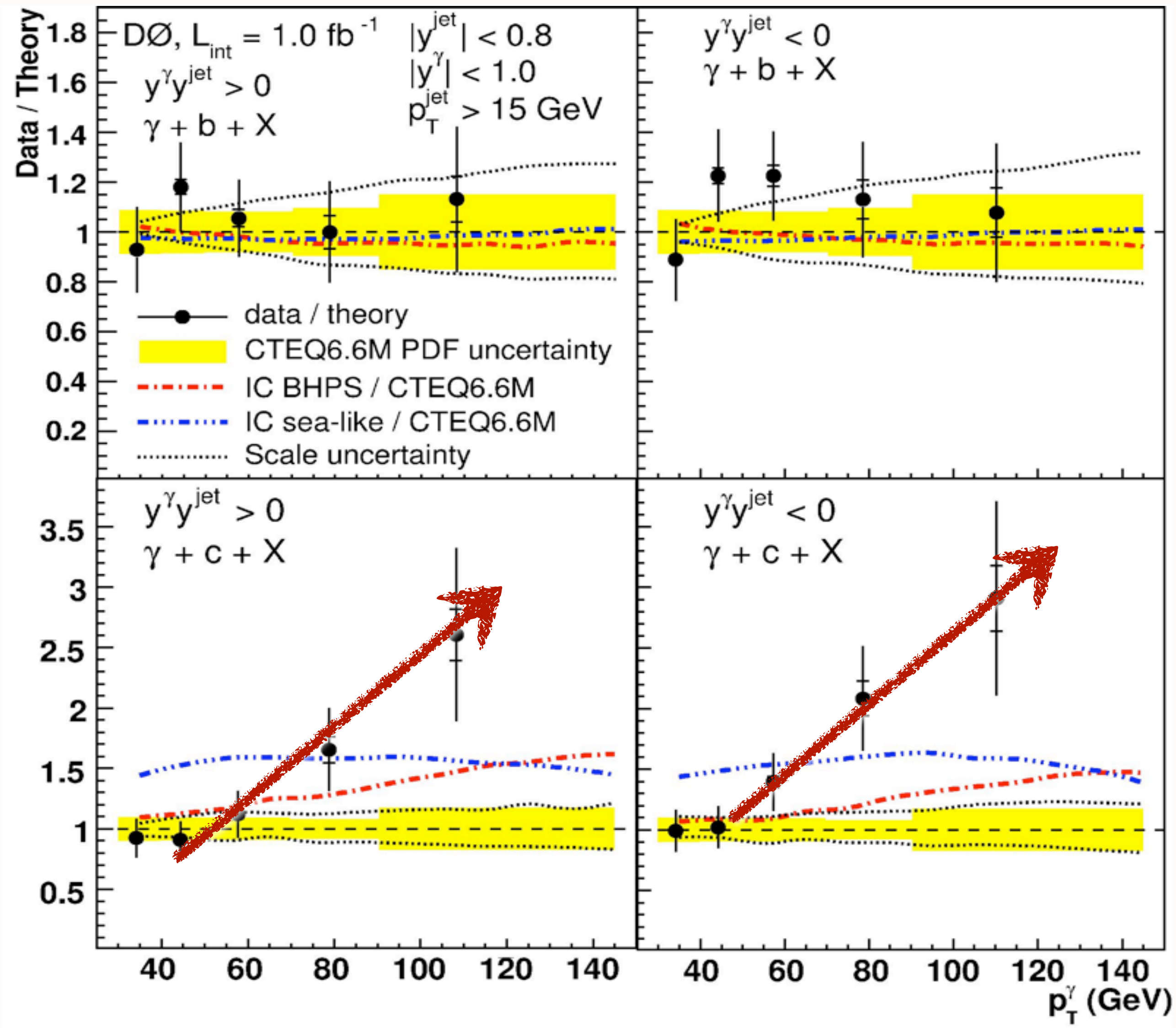

$$\frac{\Delta\sigma(\bar{p}p \to \gamma c X)}{\Delta\sigma(\bar{p}p \to \gamma b X)}$$

Ratio insensitive to gluon PDF, scales

Signal for significant IC at x > 0.1 ?

Novel Lepton Physics Studies in electron-nucleus reactions

Use JLab 4 GeV Intense Electron Beam

- Production of True Muonium $[\mu^+\mu^-]$
- Production of Relativistic Muonium $[\mu^+e^-]$
- Test All-Orders Bethe-Maximon Formula for Pair Production
- Lepton Charge Asymmetry
- Test Landau-Pomeranchuk-Migdal (LPM) Effect

Why measure Bethe-Heitler/Trident Processes?

- **Test exact all-orders Bethe-Maximon formula**
- **Test lepton\anti-lepton asymmetries**
- **Compton Effect: Spacelike and Timelike DVCS**
- **Two-photon corrections -- origin of Rosenbluth breakdown?**
- **Relativistic positronium, muonium, true muonium in flight**
- **Dissociation: LFWFs, Transparency, LPM Effect**
- **Proton size measurements; electron screening effect**
- **Muon-Proton anomaly?**
- **Fermi-Dirac Statistics**
- **QCD Analogs**